

CHALLENGES IN MEASURING θ_{jc} FOR HIGH THERMAL PERFORMANCE PACKAGES

Electronics **COOLING**

JUNE 2014
electronics-cooling.com

FEATURE

SOLDER JOINT LIFETIME OF RAPIDLY CYCLED LED COMPONENTS

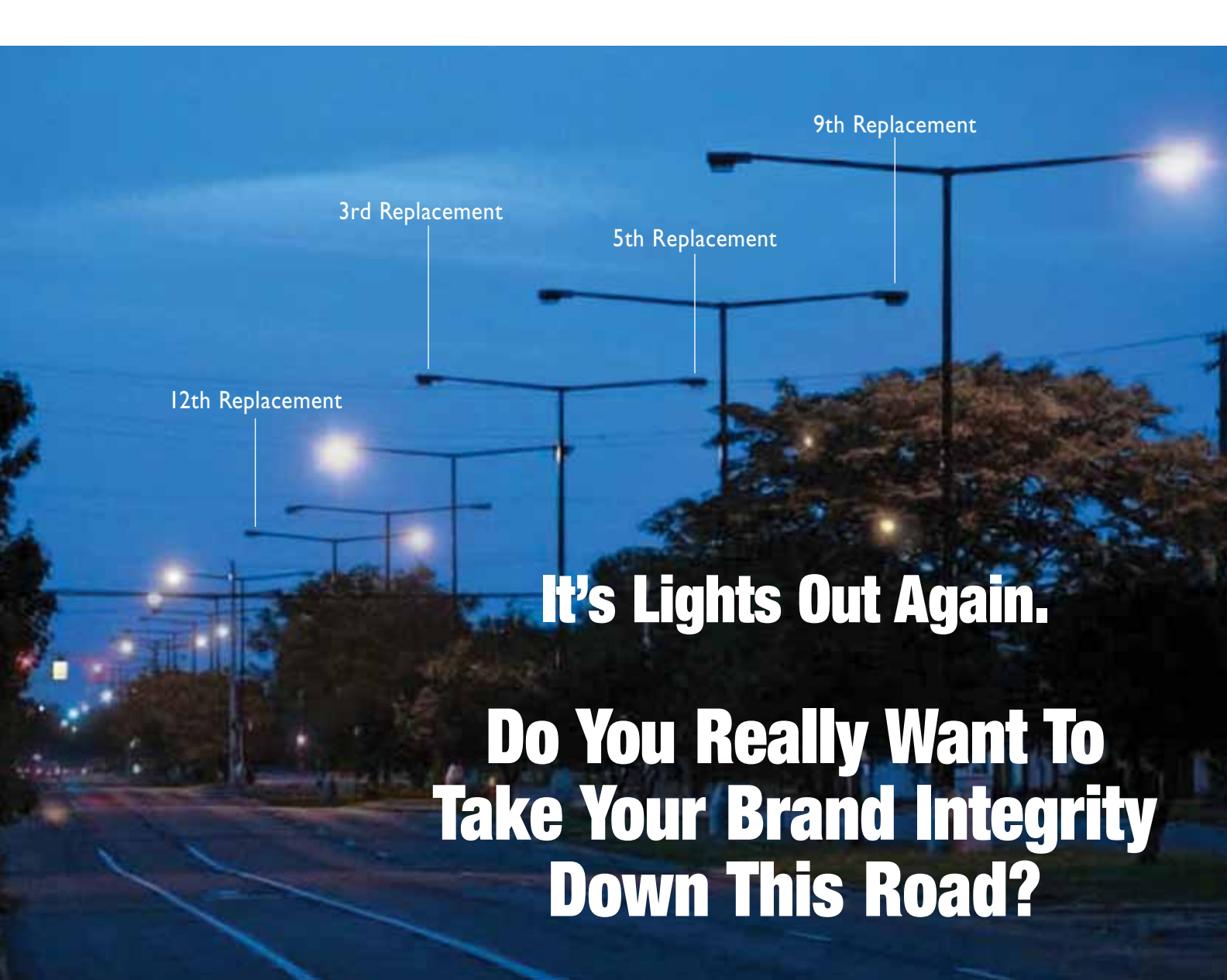
BACK COVER



INSIDE

ADVANCES IN
VAPOR COMPRESSION
ELECTRONICS COOLING

ENHANCED EDITION



It's Lights Out Again.

**Do You Really Want To
Take Your Brand Integrity
Down This Road?**

Bergquist Thermal Clad® keeps your LEDs intense, bright and reliable wherever they go.



Built for long-term reliability.

Choosing the right IMS (insulated metal substrate) can make the difference of a successful product or not. Knowing the long term performance and reliability of the materials in your design, will give your customers

a quality product and protect your reputation. This includes:

- Thermal impedance, not just thermal conductivity
- Long-term dielectric strength, not just breakdown strength
- U.L. Listed
- Long-term temperature testing

A balance of innovative thinking and expertise.

Not all substrate materials have the Bergquist company's 25+ years of testing and proven field performance. Our testing is geared to the

application, not just numbers, which give a true performance picture you can count on in your design.

Bergquist delivers cooler performance for Power LEDs.

Dielectrics: Bergquist offers a wide selection of dielectric and thickness choices to meet the demanding specs of high performance applications (Bergquist HPL and HT versions), as well as, lower performance requirements (Bergquist MP, HR T30.20 versions).

Base Plates: Bergquist offers a wide range of thicknesses, aluminum for packaged components and copper base for high power density and COB applications.

Circuit Copper: From 35µm to 350µm (1/2 oz. to 10 oz.)

Call or visit us to qualify for a FREE T-Clad Samples Kit:
www.bergquistcompany.com/coolkit



www.bergquistcompany.com 1.800.347.4572

9 5 2 . 8 3 5 . 2 3 2 2 f a x 9 5 2 . 8 3 5 . 0 4 3 0

18930 West 78th Street • Chanhassen, Minnesota 55317



Thermal Materials • Thermal Substrates • Fans and Blowers

CONTENTS

2

EDITORIAL

Bruce Guenin, Editor-in-Chief, June 2014

4

COOLING MATTERS

Prehistoric Cave Paint Shields Solar Spacecraft;
Carbon Nanotubes Boost Microprocessor Cooling and more

6

THERMAL FACTS & FAIRY TALES

Historical Suggestions for Thermal Management of Electronics
Jim Wilson, Raytheon

10

TECHNICAL BRIEF

Built-in Heat Spreading for Efficient Thermoelectric Cooling
of Concentrated Heat Loads

*Jeff Hershberger, Robert Smythe, Xiaoyi Gu, Richard F. Hill,
Laird Technologies, Inc.*

14

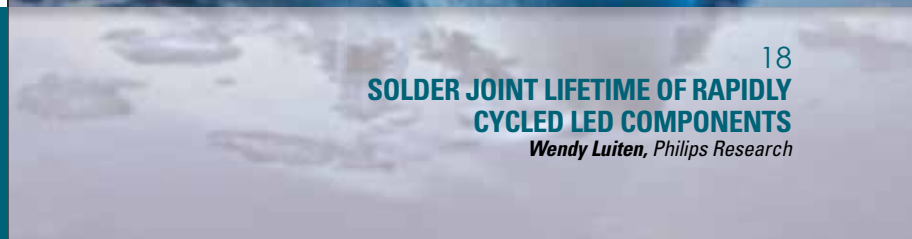
CALCULATION CORNER

Estimating the Thermal Interaction between Multiple Side
by Side Chips on a Multi-Chip Package

Je-Young Chang, Ashish Gupta, Intel Corporation



JUNE 2014



18

SOLDER JOINT LIFETIME OF RAPIDLY CYCLED LED COMPONENTS

Wendy Luiten, Philips Research

FEATURED ARTICLES

22

CHALLENGES IN MEASURING THETA JC FOR HIGH THERMAL PERFORMANCE PACKAGES

Jesse Galloway, Ted Okpe, Amkor Technology

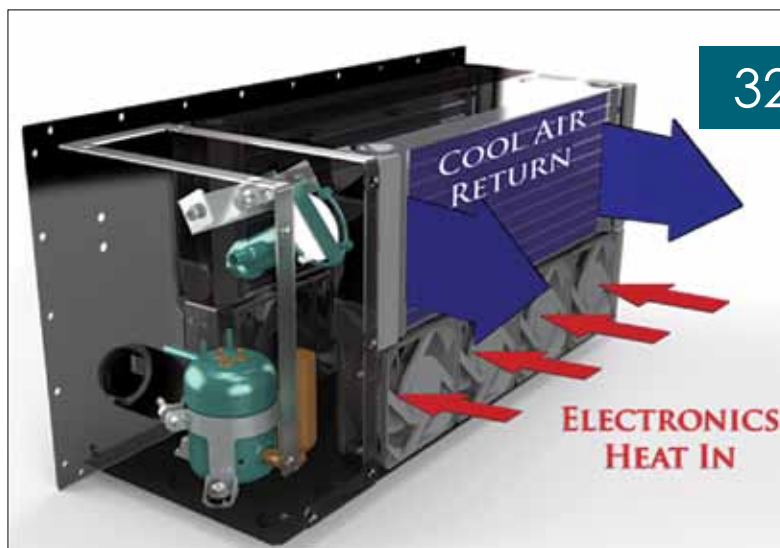
28

ADVANCES IN VAPOR COMPRESSION ELECTRONICS COOLING

James Burnett, Aspen Systems

32

INDEX OF ADVERTISERS



32

Editorial

Globalization, Artificial Intelligence, and the Future of Thermal Engineering

Bruce Guenin, Editor-in-Chief, June 2014



MANY SOCIAL AND ECONOMIC COMMENTATORS reminisce about the post-World War II boom. It was fueled in part by the rebuilding of national infrastructures but also by significant developments in the automation of the means of production. This led to a virtuous cycle of: automation leading to higher productivity per worker => a climate of general prosperity => creation of new industries requiring new workers.

In contrast, as we consider our own era, we are continually reminded by the headlines of the problems with unemployment, underemployment, and wage stagnation. We struggle to make sense of this situation and try to reconcile it with the sense of optimism we had in the past.

Our age, in many ways, offers opportunities for entrepreneurial engineers that were not available in the past. Those who endeavor to create companies providing software services, can rent the required computing resources from one of the several cloud computing providers, rather than creating their own data center. Furthermore, they can hire contract programmers, that may even be in other countries. Companies that manufacture products can function effectively as highly streamlined design and marketing operations with the actual fabrication performed offshore by contract manufacturers. These structural efficiencies greatly reduce the need for capital in the creation of these companies than in years past and tend to lower the cost of their products. The result is that they also would tend to hire fewer employees than would have been the norm in former times.

Another change is that we are seeing more examples of software demonstrating artificial intelligence, performing activities that were previously considered to require human reasoning and judgment. Examples are legal research, the more routine aspects of IC circuit design, medical diagnosis, accounting, and tax preparation. It is an inevitability that the further development of artificial intelligence will encroach on other disciplines.

In the face of these profound changes it behooves each of us to assess the potential impact of artificial intelligence on our own job security and change our value proposition accordingly. It should be noted that the jobs that are most vulnerable to being automated are those that can be reduced to the execution of a series of rules. Hence, it is likely that the process of performing a computer simulation of heat transfer in an electronic system will become more and more automated over time. In contrast, those activities that use our more expansive mental capabilities to span different engineering disciplines or to create novel solutions to problems should be less at risk. An example of the former would be that, once the thermal behavior is determined by simulation, the engineer takes the calculation to the next level by determining the reliability implications of the calculated temperatures, and, if necessary proposes changes to the design to address any reliability shortfall. Of course, when it comes to product innovation, the creative capabilities of the human mind far exceed those of computers at the present time.

I think that it is fair to say that, in the future, thermal engineers seeking career success will need to add an additional dimension to their value proposition. It could be that of an entrepreneur, either as a creator of a business or an enterprising contractor, providing thermal engineering services to a number of clients. Alternatively, for engineers with a more purely technical focus, it could be coupling thermal analysis to a second discipline whose domain is critical to the successful functioning of a product. Of course, there will always be opportunities for thermal engineers who can create game-changing innovations to neutralize critical thermal problems.

Electronics COOLING

www.electronics-cooling.com

ASSOCIATE TECHNICAL EDITORS

Bruce Guenin, Ph.D.
Principal Hardware Engineer, Oracle
bruce.guenin@oracle.com

Madhusudan Iyengar, Ph.D.
Thermal Engineer, Google
miyengar@gmail.com

Peter Rodgers, Ph.D.
Professor, The Petroleum Institute
proddgers@pi.ac.ae

Jim Wilson, Ph.D., P.E.
Engineering Fellow, Raytheon Company
jsw@raytheon.com

PUBLISHED BY

ITEM Media
1000 Germantown Pike, F-2
Plymouth Meeting, PA 19462 USA
Phone: +1 484-688-0300; Fax: +1 484-688-0303
info@electronics-cooling.com; electronics-cooling.com

CONTENT MANAGER

Belinda Stasiukiewicz
bstas@item-media.net

BUSINESS DEVELOPMENT MANAGER

Casey Goodwin
cgoodwin@item-media.net

GRAPHIC DESIGNER

Evan Schmidt
eschmidt@item-media.net

ASSISTANT EDITOR

Aliza Becker
abecker@item-media.net

PRESIDENT

Graham Kilshaw
gkilshaw@item-media.net

REPRINTS

Reprints are available on a custom basis at reasonable prices in quantities of 500 or more. Please call +1 484-688-0300.

SUBSCRIPTIONS

Subscriptions are free. Subscribe online at www.electronics-cooling.com. For subscription changes email info@electronics-cooling.com.

All rights reserved. No part of this publication may be reproduced or transmitted in any form or by any means, electronic, mechanical, photocopying, recording or otherwise, or stored in a retrieval system of any nature, without the prior written permission of the publishers (except in accordance with the Copyright Designs and Patents Act 1988).

The opinions expressed in the articles, letters and other contributions included in this publication are those of the authors and the publication of such articles, letters or other contributions does not necessarily imply that such opinions are those of the publisher. In addition, the publishers cannot accept any responsibility for any legal or other consequences which may arise directly or indirectly as a result of the use or adaptation of any of the material or information in this publication.

Electronics Cooling is a trademark of Mentor Graphics Corporation and its use is licensed to ITEM. ITEM is solely responsible for all content published, linked to, or otherwise presented in conjunction with the Electronics Cooling trademark.





Electronics cooling heat sink

Malico is not an "Ordinary" Company
We are a "Unique" and "Driven" family
Malico does not chase profits, instead we chase Zero Defects.
Quality is engineered into every part we make.
Our Customers count on Malico's reliability and advanced solutions capabilities.
Bring us your requirements and let us show you how we can both succeed!



Malico Inc.

5, Ming Lung Road, Yangmei, 32663 Taiwan
Tel : 886-3-4728155
Fax: 886-3-4725979
E-mail: inquiry@malico.com
Website: www.malico.com

Cooling Matters

Applications of thermal management technologies

DIAMOND-MINERAL OIL MIX MAY BE BEST HEAT TRANSFER NANOFLUID

A mixture of diamond nanoparticles and mineral oil may be the most effective nanofluid for heat transfer applications, according to new research from Rice University.

Since the late 1990s, researchers have been experimenting with nanosized particles in low concentrations in order to create a nanofluid that offers a middle ground between flow and thermal transport properties. According to the Rice University team, nanodiamonds have proven to be the best additive yet, offering 100 times better thermal conductivity than copper while still acting as an efficient lubricant.

In tests, the Rice scientists dispersed nanodiamonds in mineral oil and found that a small concentration—one-tenth of a percent by weight—raised the thermal conductivity of the oil by 70 percent at 373 kelvins (211°F). Dispersing the same amount of nanodiamonds at a lower temperature of 323 K still raised the thermal conductivity, albeit a smaller increase of about 40 percent.

Source: Applied Materials and Interfaces

POLYMER-BASED THERMAL INTERFACE MATERIAL COOLS DEVICES AT 200°C

Scientists have developed a new polymer-based thermal interface material capable of conducting heat 20 times better than conventional polymer. Reliable in temperatures of up to 200°C, the modified material can be fabricated on heat sinks/heat spreaders and adheres well to components in servers, LEDs and mobile devices.

Developed by researchers from the Georgia Institute of Technology, University of Texas and Raytheon Company, the new modified TIM is produced from polythiophene. Polythiophene is a conjugated polymer in which aligned polymer chains in nanofibers facilitate the transfer of phonons, but without the brittleness associated with crystalline structures. The formation of the nanofibers produces an amorphous material with thermal conductivity of up to 4.4 W/(m•K).

Researchers have tested the new polymer-based TIM up to 200°C, a temperature range suitable for various automotive applications. The material could also enable reliable thermal interfaces to be as thin as three microns, making it ideal for use in microelectronics.

The technique still requires further research and development, but it could be eventually scaled up for manufacturing and commercialization.

Source: Georgia Institute of Technology

THERMOELECTRIC GENERATOR COULD POWER WEARABLE DEVICES WITH BODY HEAT

A glass fabric-based thermoelectric generator that is extremely light and flexible and produces electricity from the heat of the human body has been created by researchers at the Korea Advanced Institute of Science and Technology (KAIST).

Currently, two types of thermoelectric generators exist. Organic-based thermoelectric generators use flexible polymers that are compatible with human skin, but have a low power output. Inorganic-based thermoelectric generators produce adequate electrical energy, but are bulky. The new technique balances the two, yielding a flexible thermoelectric generator that minimizes thermal energy loss while maximizing power output.

Tests indicate KAIST's thermoelectric generator will produce around 40 mW electric power based on a temperature difference of 31°F between human skin and the surrounding air.

Source: KAIST



Datebook

JUNE 2-5

Thermal Imaging Conference 2014

LAS VEGAS, NEV., US
www.thermalimagingconference.com

JUNE 16-20

11th AIAA/ASME Joint Thermophysics and Heat Transfer Conference

ATLANTA, GA, US
www.aiaa.org/EventDetail.aspx?id=18644

JULY 6-10

International Conference on Thermoelectrics

NASHVILLE, TENN., US
<http://web.ornl.gov/sci/theory/ict2014>

AUGUST 4-8

NASA Thermal and Fluids Analysis Workshop

CLEVELAND, OHIO, US
<https://tfaws.nasa.gov>

PREHISTORIC CAVE PAINT TO SHIELD SOLAR SPACECRAFT

A European spacecraft scheduled for launch towards the Sun in 2017 will be shielded from extreme temperatures by a type of paint once used in prehistoric cave art.

Carrying instruments to perform high-resolution imaging of the sun, the European Space Agency's Solar Orbiter will travel as close as 42 million kilometers from the Sun—the closest a spacecraft has ever been to the star.

According to ESA officials, burnt bone charcoal, a type of pigment once used by early humans to create art on the walls of caves in France, will be applied to the spacecraft's titanium heatshield to help protect it from extreme conditions. Operating in direct view of the Sun, the mission will be exposed to 13 times the intensity of terrestrial sunlight and temperatures as high as 520°C.

The decision to include the burnt bone charcoal in the design was made after ESA scientists realized that conventional manufacturing methods and materials would not be able to meet requirements for the heatshield.

Source and image: European Space Agency



CARBON NANOTUBES BOOST MICROPROCESSOR COOLING

Researchers from the U.S. Department of Energy have developed a new technique that combines carbon nanotubes and organic materials to enable more efficient cooling of microprocessor chips.

While carbon nanotubes have long been known to offer high thermal conductivity, widespread application in cooling systems has proven difficult because of their high thermal interface resistance.

Now, researchers claim to have solved this issue using organic compounds to form strong covalent bonds between carbon nanotubes and the metal surface of the chip. The resulting thermal interface material conducts heat six times more effectively.

In addition, the new bonding technique adds just seven microns on each side of the CNT layer during the bonding process, compared to older methods that add 40 microns.

Source: Nature Communications

GRAPHENE IMPROVES COPPER FILM THERMAL CONDUCTIVITY

The placement of a single atomic plane of graphene on the surface of a copper film can significantly increase the film's thermal conductivity, making the hybrid material ideal for more demanding thermal management applications.

The phenomenon was discovered while studying how thermal properties of copper films change as graphene synthesized by chemical vapour deposition (CVD) is placed on top of the films. The results are from changes in the copper's morphology rather than from the graphene acting as an additional heat-conducting channel.

This increase in grain size is larger than in reference copper films that were simply heated to the same temperatures as those employed in the CVD process. The larger copper grain size, coupled with the graphene coating, results in higher thermal conductivity.

Source: University of California Riverside

MAGNETIC-STIMULATED FLOW PATTERNS BOOST HEAT TRANSFER

Magnetically-stimulated fluid flow patterns may offer a new method for handling difficult heat transfer problems by overcoming natural convection limits.

Kansas State researchers have discovered a new technique that could be useful for cooling in microgravity or for transferring heat in circumstances that prevent convection. Known as isothermal magnetic advection, the new technique makes fluids move without mechanical assistance through the addition of a small amount of magnetic platelets to the liquid and the application of modest, uniform alternating current magnetic fields.

The platelets are initially dispersed randomly throughout the liquid, but quickly form into patterns when a magnetic field is applied.

Source: Kansas State

AUGUST 6-7

Advancements in Thermal Management 2014

DENVER, COLO., US
www.thermalnews.com/conferences

SEPTEMBER 9-11

PCB West SANTA CLARA, CALIF., US

<http://pcbwest.com>

SEPTEMBER 14-17

42nd Annual Conference of NATAS

SANTA FE, N.M., US
www.natasinfo.org/conferences/2014-42nd-annual-conference

SEPTEMBER 16-18

The LED Show LOS ANGELES, CALIF., US

www.theledshow.com

Historical Suggestions for Thermal Management of Electronics

Jim Wilson, Engineering Fellow, Raytheon Company

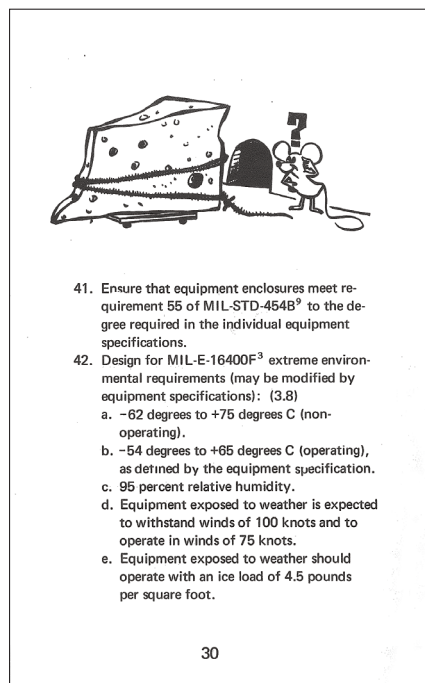
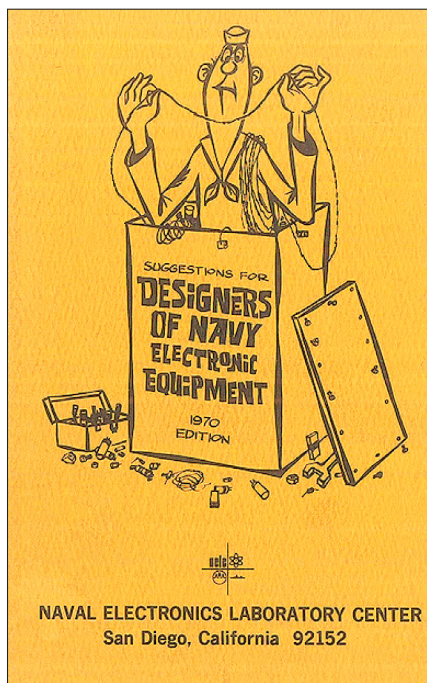
HAVE A SMALL book in my office labeled “Suggestions for Designers of Navy Electronic Equipment, 1970 Edition” and it was given to me several years ago by the editor at microwaves101.com (which happens to be a useful website if you are interested in microwave topics). The introduction states that any or all of this information is reproducible as long as credit lines are given, so a few pages related to thermal management (including the nice illustrations) are reproduced in this column.

An appropriate fact would be that thermal issues with electronics have been around as long as we have had electronics, but despite the long history of thermal management hardware and packaging solutions, it would be a fairy tale to think that cooling of electronics is easy. The suggestions in the book cover a range of topics that were of interest to end users of that time period such as design and reliability.

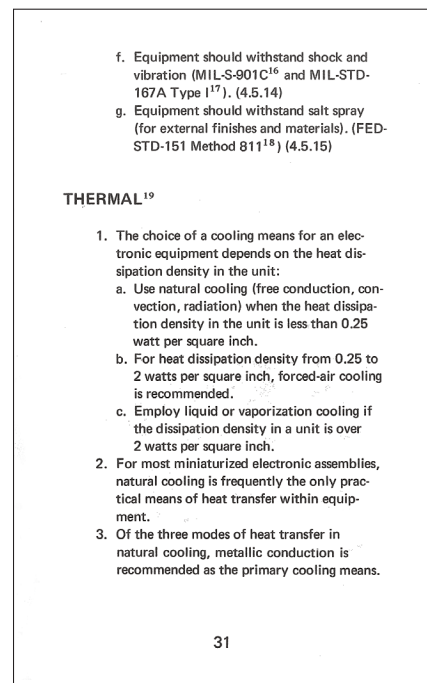
The book has 99 suggestions in the thermal section and perhaps not surprisingly, some of them still ap-

ply. This information was compiled before modeling and simulation was common or even practical with the computational resources of that time period.

Expectations in 1970 relied on following generally accepted design practices and validation testing. Reasonable expectations of today are usually much more comprehensive and include simulations and confirmation tests. Densely packaged electronics with high heat loads that are common today would be difficult, if not impossible, to design

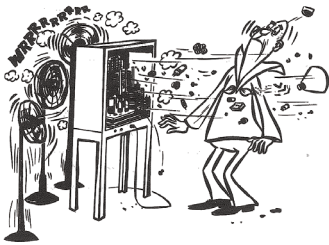


30



31

4. For electronic equipment designed to operate in thermal environment of high ambient temperature or with high heat dissipations, liquid or vaporization cooling is best.
5. Base the design of forced-air cooling systems on the volume and weight of the equipment, the attainment of safe operating temperature at the heat sources, and the minimization of cooling power; i.e., the energy requirement for moving the air through the cooling system.



32

6. Limit heat dissipation by choosing efficient parts (semiconductor devices instead of electron tubes, for example) and circuits (class B or C operation instead of class A).
7. Use parts which have maximum thermal operating range and minimum temperature sensitivity.
8. Design circuits to be as tolerant of temperature range as possible. NEVER assume that a design will be satisfactory over the range of temperatures required of military equipment on the basis of tests performed at room ambient temperature on a development bench.
9. Design equipment so that heat flow paths are the result of planned effort in order that thermal performance may be subject to manufacturing control in the same manner as electrical performance.

NATURAL COOLING^{20, 21}

10. Use heat flow paths of lowest possible thermal resistance.
11. Ensure that heat flow paths are as short as possible, have large cross-sectional areas, and are made of material having good thermal conductivity.

33



12. Arrange hot components to form a bank of minimum height.
13. Use heavy metal chassis for conducting heat.
14. Stagger parts where vertical stacking is used.
15. Make sure all joints conduct heat well and are close fitting to provide a maximum metal-to-metal contact. Where necessary, silicon greases are recommended for use in improving joint conductivity.
16. Isolate from or place below heat sources all temperature-sensitive components.
17. Provide polished and unpainted heat shields for heat-sensitive components located less than 2 inches from heat source.
18. Mount all parts which dissipate more than 1/2 watt on metal chassis or provide them with heat paths leading to a heat sink.

34

19. Provide ventilation louvers of proper design and location that will provide a drip-proof enclosure where required.
20. Make sure that heat sources have high emissivity and, if embedded, are provided with metal heat conductors.

FORCED-AIR COOLING²²

21. Direct cooled, filtered air to the hot parts.
22. Avoid reuse of cooling air. If secondhand air or series-flow air must be used, the sequence of air passage over cooled parts must be carefully planned so that temperature-sensitive parts or parts with low maximum permissible operating temperatures are cooled first, and so that the coolant has sufficient thermal capacity to maintain required temperature for all parts.
23. Cool hot parts by parallel air flow.
24. Insure the air flow paths are free and unobstructed and are of proper size.
25. Insure that intakes and exhausts are far apart.
26. Design so that the blower capacity is adequate and blower motor is cooled.
27. Verify air flow in equipment by measuring and mapping with smoke.
28. Make air filters adequate and accessible for easy cleaning and replacement.
29. Consider protecting against equipment damage in case of blower failure.
30. Insure that power tubes have required air flow.

35

31. Minimize air-flow noise.
32. Measure the critical temperatures and protect fragile fins.
33. Design to have the air flow first pass over the seals of critical tubes.
34. Design so that forced convection is in a direction to aid the natural convection.
35. Include in air-flow calculations area reduction caused by wiring (including ship wiring) in the air ducts.
36. Do not locate ventilation openings at enclosure top, bottom, or front surfaces without specific approval.

LIQUID COOLING²³



36

37. Obtain approval of the command or agency concerned if liquid cooling is used.
38. Design so that the coolant can expand freely and the enclosure can withstand the maximum vapor pressure of the coolant.
39. Be sure that the piping is adequate and equipment is hermetically sealed.
40. Provide adequate drains and filter plugs.
41. Design equipment so that drains are at low points and bleeder valves are at high points of the system.
42. Insure that the heat exchangers are of proper design and capacity.
43. Insure that the coolant does not boil below maximum temperature and, if necessary, provide a temperature control device.
44. Avoid condensation of moisture in the equipment. But if it happens to be unavoidable, a pressure of nearly one atmosphere should be maintained outside of the enclosure.
45. Use a check valve at each disconnection.
46. Orient and mount parts to achieve maximum convection.
47. If feasible, design to provide metallic conduction paths of low thermal resistance from heat sources to the case; although they are not essential, they are very helpful and do not require special attention.
48. In designing the cooling assembly always remember the aspects of maintenance and repair.

37

without thermal simulation tools (and a thermal engineer to generate and interpret results).

The thermal section starts with rough guidelines on selecting natural, forced air, liquid or two-phase cooling based on heat flux. Advances in packaging and heat sink designs have made air and liquid cooling feasible at higher heat flux levels for both free and forced convection.

General guidelines to consider when designing for natural, forced air, liquid, or vaporization cooling follow. The last suggestions are related to different types of electronics and while not many of us deal with tube cooling today, it is interesting to look at the integrated and other semiconductor devices section. Suggestion number 84 states that the thermal design of ICs are critical. This

VAPORIZATION COOLING²³

(Factors applicable to liquid cooling apply here also.)

49. Be sure that sufficient coolant is provided.
50. If required, install a make-up reservoir.
51. Prevent toxic fumes from reaching personnel.
52. Provide pressure control and pressure relief valves.
53. Conduct environmental tests on refrigeration systems.

COOLING OF TUBES⁸

54. Position electron tubes so as to avoid the formation of hot spots.
55. Space unshielded tubes at least 1-1/2 diameter apart.
56. Screen tubes from each other; do not pot tubes in plastics.
57. Avoid direct radiation from electron tubes.
58. Avoid running tube anodes red hot.
59. Verify that the bulb temperatures are within specification.
60. Protect tubes from mechanical injury.
61. Use thermocouples or temperature sensitive paints to investigate thermally critical tube applications.

TUBE SHIELDS

62. Use nonmagnetic heat dissipating shields on all miniature and subminiature tubes. (3.4.33)
63. Make shields fit the tubes tightly; use non-precious metals.

38

64. Choose shields that are highly emissive and thermally conductive to the chassis.
65. Provide low-resistance metal joints.
66. Avoid mounting heat-conducting shields on plastic chassis.
67. Use shields that have been blackened internally and polished externally.

RESISTORS (which dissipate more than 1/10 rated power)

68. Bond resistors to the panel or chassis by a clamp of low thermal resistance.
69. Do not place resistors adjacent to heat-sensitive components.
70. Mount power resistors vertically in groups. Similarly mount other resistors over 5 inches long.
71. Mount resistors so that leads are as short as possible.
72. Design to allow air to flow freely over resistors.
73. Derate resistors if environmental temperatures are high, in accordance with tables established in the applicable specifications. A minimum derating of 50 percent is normal.
74. Locate composition resistors, such as those used in feedback loops or bridge-balancing networks, in comparatively cool areas.
75. Place bleeder resistors adjacent to cabinet or chassis surfaces that provide good thermal sinks.

39

CAPACITORS

76. Isolate heat-sensitive capacitors from hot components.
77. Provide radiation shields.
78. If possible, use capacitors or relatively low-heat-sensitivity materials.

TRANSFORMERS AND INDUCTORS

79. Provide transformers and chokes with clean low-resistance thermal joints to heat-conducting chassis.
80. Keep transformers potted and enclosed.
81. Provide adequate heat dissipation surface areas and good thermal conductivity between the windings and case.
82. Make sure that thermal joints are free of impregnant and paint.
83. Isolate temperature-sensitive inductors from heat sources; if possible, locate them near a cabinet or other metallic thermal sink.

INTEGRATED CIRCUITS AND OTHER SEMI-CONDUCTOR DEVICES

84. Remember that semiconductor devices are usually very heat sensitive. Thus, their thermal designs are critical.
85. If power transistors or power rectifiers are used, provide connections of low thermal resistance to well-cooled, heat-conducting chassis.

40

86. Keep temperature environment as nearly constant as possible.
87. Clamp transistors dissipating more than 100 milliwatts to a chassis or heat sink.
88. Mount power rectifiers in a cool place and provide them with large, vertical fins.
89. Design to insure that semiconductor devices will not deteriorate in performance with increasing temperature.
90. The use of solder is preferred for mounting of integrated circuits to boards. In any case, sockets should not be used because of their unreliability. The use of welding is not recommended since repairs often damage circuit board conductors and in addition create quality control problems related to welding schedules, etc.
91. Mount integrated circuits so that the case firmly contacts the mounting surface to provide heat sinking.
92. Do not mount integrated circuits by suspending them from their leads.
93. Do not rely entirely on heat sinking. Integrated circuits require additional cooling.

41

94. Use only integrated circuits with gold-plated leads. In addition, the leads must have been plated prior to sealing the case. The use of conformal coatings to seal assemblies is encouraged, since leads are generally Kovar and rust rapidly. Consideration must be given to use of coatings which will facilitate repair if this is part of the maintenance philosophy.
95. Critically screen manufacturer's electrical parameter values, as these values quite frequently are unrealistic and optimistic. It is recommended that circuits be tested to determine typical values.
96. Do not load integrated circuit outputs to more than 70 percent of manufacturer's maximum fanout ratings.
97. Do not exceed the manufacturer's recommended power supply voltage. Maximum ratings should never be used. Guard against electromagnetic interference by use of appropriate shielding. Integrated circuits are susceptible to and create noise.
98. Do not use edge board connectors with less than 0.100 inch contact spacing for mounting integrated circuits. Less spacing provides insufficient contact area and reduces reliability.

42

99. The use of wire-wrap in accordance with MIL-STD-1130²⁴ provides acceptable back plane wiring. Solder terminations with sufficient quality control generally result in acceptable wiring. Any other termination should be subjected to critical screening through environmental evaluations, as well as maintenance tests prior to selection and usage.

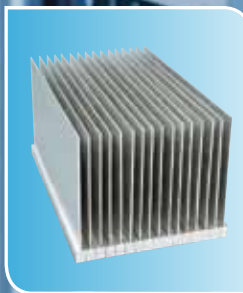
43

statement has proven to be true and is one of the main focus topics of electronics cooling. Suggestion 95 comments on validating parameters listed in manufacturer's data sheets as they were found to be unreliable. Today, 45 years later, this is still good advice.

In the field of electronics thermal management, we

have significantly more design capability today than existed when this book was compiled. However, a good lesson for all of us is to remember that this book was written from the end user's viewpoint. We should make sure that considering the customer's perspective in our thermal management designs has a high priority.

Aluminum extrusions make the difference



Advanced aluminum extrusion solutions for thermal management

When powerful technology gets smaller, things can really heat up. How do today's leading companies develop designs that look great and solve the thermal management problem? Thanks to a higher level of thermal conductivity, aluminum extrusions can be as much as 53% more efficient than aluminum castings. In addition, Sapa has developed a new method of manufacturing high ratio air cooled heat sinks. Our new technique uses Friction Stir Welding (FSW) technology in

a modular concept allowing for maximum flexibility and fin ratios in excess of 40:1. FSW also allows for the production of large scale heat sinks up to 20" wide.

With complete thermal engineering and design assistance plus full fabrication capabilities at multiple locations across North America, Sapa can provide finished component heat sinks for all of your needs.

Contact us for more about Sapa and thermal:

NorthAmerica.Sales@sapagroup.com
(877) 710-7272



www.sapagroup.com/NA

Built-in Heat Spreading for Efficient Thermoelectric Cooling of Concentrated Heat Loads

Jeff Hershberger, Robert Smythe, Xiaoyi Gu, Richard F. Hill
Laird Technologies

INTRODUCTION

THERMOELECTRIC cooling is an active thermal management technique. A thermoelectric cooler (TEC) has two circuit boards which are typically Al_2O_3 plates with copper circuit

traces attached to them and semiconductor elements soldered between them. TECs are now available where these Al_2O_3 -based circuit boards have been replaced with Thermally Conductive Printed Circuit Boards (TCPCBs). TCPCBs are laminates consisting of a metal backing plate

(in this study, 0.64mm thick copper), a layer of thermally conductive filled polymer for electrical isolation and a copper foil that can be etched into circuit patterns using standard PCB processes. The thermally conductive filled polymer consists of a fully cured epoxy and a high volume loading of different sizes of ceramic particles such as Al_2O_3 . Figure 1 is a photograph of the two types of TECs compared in this study [1].

In a TEC with a concentrated heat load, i.e. one smaller than the TEC, the semiconductor elements far from the heat load still consume electrical power but contribute less heat pumping, leading to reduced efficiency [2]. This occurs because the aluminum oxide circuit boards are thin (< 1 mm) and have limited thermal conductivity (~30 W/mK) and therefore offer limited heat spreading. Thicker aluminum oxide circuit boards would provide better heat spreading but would have higher through-thickness thermal resistance. In some applications, additional heat spreading is provided by the inclusion of a metal or ceramic plate between the heat load and the TEC, but this added component increases cost and complexity and makes quality control more difficult. The use of TCPCBs in TECs seeks to provide heat spreading without these drawbacks by decoupling the through-thickness thermal resistance from the in-plane heat spreading. In this paper, we demonstrate that TCPCB-based TECs provide better efficiency than Al_2O_3 -based TECs when cooling concentrated heat loads.

Jeff Hershberger is a senior scientist at Laird, where he has worked for seven years on development of thermoelectric materials and modules. His Ph.D. is in Materials Science with specialties in X-ray techniques and thin films. He was previously Staff Scientist at the Energy Technology Division of Argonne National Laboratory. Jeff recently relocated his family from Cleveland, Ohio to Durham, North Carolina and is looking forward to warmer weather.



Bob Smythe is the director of manufacturing engineering for Laird Engineered Thermal Systems business. He has over 20 years' experience in thermoelectric technology and business development. Bob was educated at The College of New Jersey and Rider University, with a BSc. in Biology and a US Army commission. He is an inventor on several U.S. patents related to thermal technologies.



Xiaoyi Gu is the Manager of Technology Group at Laird where he has worked over 10 years on Thermoelectric material and module development, new process development, reliability and failure analysis. He has over 40 years' experience in technology and process development in the areas of silicon material & devices, gallium arsenide & devices, PWB/PCB, quartz crystal & oscillators and thermoelectrics. Xiaoyi received BS in Chemistry from Fudan University, China and is located at Shenzhen, China now. Xiaoyi is an inventor on several Chinese & U.S. patents.



Richard Hill joined Laird in 1999 where he is currently the vice president of technology for the Performance Materials business. He has more than 40 years' experience in technology and new business development in the areas of zeolites, aluminas, barium titanate, ceramic materials for electronics and non-oxide powders and shapes (Union Carbide); polymer-ceramic composites (Advanced Ceramics and University of New Mexico); and thermal, thermoelectric materials, EMI, RF absorbers and ferrite ceramic inductors (Laird). Hill's educational background includes a BS in Ceramic Engineering and an MS in Ceramic Science, both from Rutgers University in his home state of New Jersey, and a Doctorate degree in Materials Science from the University of Leoben in Austria. Hill is inventor on over 20 U.S. patents.



INTRODUCING COOLSPAN® TECA

thermally & electrically conductive adhesive

Rogers can help by being your reliable conductive adhesive film source

Get the heat out of those high-power PCBs. COOLSPAN® Thermally & Electrically Conductive Adhesive (TECA) Films are ideal for dissipating heat in high-frequency circuits. COOLSPAN adhesives feature outstanding thermal conductivity (6 W/m/K) and reliable thermal stability. Keep things cool, with Rogers and COOLSPAN TECA film.

CONTACT YOUR
SUPPORT TEAM
TODAY



Visit Us At
International Microwave Symposium
3-5 June 2014 • Tampa Bay, Florida
Booth #1833



Advanced Circuit Materials Division

www.rogerscorp.com

MEET YOUR COOLSPAN® TECA FILM SUPPORT TEAM

Leading the way in...

• Support • Service • Knowledge • Reputation

SCAN THE CODE TO GET OUR CONTACT INFO.



Greg Bull
Applications
Development
Manager
Northern
Territory
(U.S.) &
Canada



Dale Doyle
Applications
Development
Manager
Western
Territory
(U.S.)



John Dobrick
Applications
Development
Manager
Southern
Territory
(U.S.) & South
America



Scott Kennedy
Applications
Development
Manager
Eastern
Territory (U.S.)



John Hendricks
European Sales
Manager



Kent Yeung
Regional Sales
Director Asia

If you are unable to scan a VR code please visit our
Support Team website at www.rogerscorp.com/coolspan

EXPERIMENT

Measurements of coefficient of performance (COP) were performed using a DX8020 TEC Expert system manufactured by RMT Ltd [3]. A schematic of this system is shown in Figure 2 and the dimensions of relevant components are given in Table 1. This system provided a controlled temperature for the hot side of the TEC, variable current and measurement of voltage to the TEC, variable heat load to the controlled side of the TEC and measurement of the temperature of the controlled side of the TEC in a vacuum environment at $\sim 1.3 \times 10^{-2}$ Pa ($\sim 10^{-4}$ Torr). The system also provided automatic corrections for heat flow in and out of the controlled side of the TEC by radiation and conduction through the wires. We added a mechanism to press the components down onto the baseplate and the system did not provide corrections for conduction through this structure. We have attempted to minimize that uncorrected heat flow by constructing the mechanism out of a polymer screw sharpened to a point. In this work, the heat load was delivered to the controlled side of the TEC through one of two experimental heat spreaders. A small experimental heat spreader with a trapezoidal cross section was used to simulate a concentrated heat load $\sim 25\%$ the width of the TEC, while a large experimental heat spreader (the same size as the TEC) was used to simulate

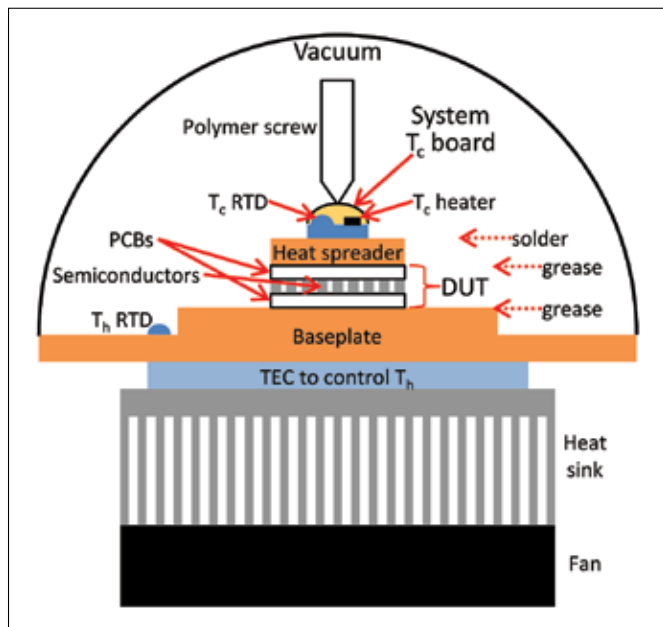


FIGURE 2: Schematic of the test system. From the bottom up, the test system consisted of a fan and heat sink removing heat from a TEC that was used to control the temperature of the system's copper baseplate. The hot side temperature was measured by an RTD next to the sample mounting area. The device under test (DUT) consisted of PCBs and semiconductors and was mounted on the baseplate using thermal grease. The experimental heat spreader was mounted on top of the DUT using grease. The system's T_c board was soldered to the top of the heat spreader. The system T_c board consisted of an RTD and a heater on a TCPCB covered by protective epoxy. The system T_c board was pressed down by a sharpened polymer screw.

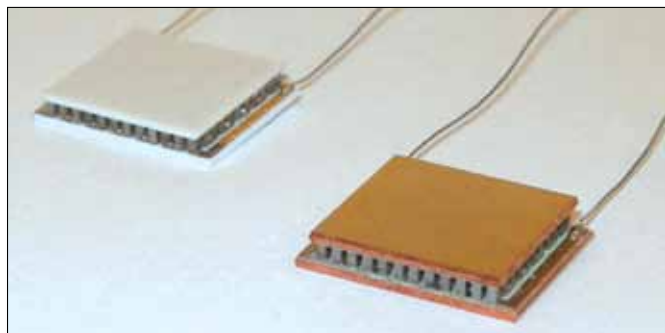


FIGURE 1: TECs with Al_2O_3 -based (left) and TCPCB-based (right) circuit boards.

uniform heat loads. The size of the small experimental heat spreader was chosen to be comparable to the sizes of common heat-producing components such as laser diodes.

To compare COPs from different TECs and configurations, we used the same heat load Q_{ctest} , cold side temperature T_c and hot side temperature T_h in all tests. We chose $T_h = 25^\circ\text{C}$ and $\Delta T = T_h - T_c = 30^\circ\text{C}$ arbitrarily, and then chose a heat load $Q_{\text{ctest}} = 1.784$ W which is equal to 80% of the maximum value typically achievable under those conditions. The TEC leads were soldered to the system's control board, it was mounted on the baseplate using thermal grease, the experimental heat spreader was mounted on top of it using thermal grease, and the system was evacuated. At the chosen values of T_h , ΔT and Q_{ctest} , the TEC drive current I and voltage V were recorded. The COP was then calculated as follows [4]:

$$\text{COP} = \frac{Q_{\text{ctest}}}{VI}$$

RESULTS AND DISCUSSION

The COP was measured for four different configurations in this work. The small experimental heat spreader was installed in the test system and this concentrated heat load configuration was used to test five Al_2O_3 -based TECs and five TCPCB-based TECs. Then, the large experimental heat spreader was installed in the system and this uniform heat load configuration was used to retest the same ten TECs. See Figure 3 for photographs of two of these configurations. The average COP, TEC current, and TEC voltage results are listed in Table 2.

RESULTS UNDER UNIFORM HEAT LOADING

As expected, in both cases with uniform heat loading, the TEC circuit was more efficient (higher COP) than in the cases with concentrated heat load. The difference in COP between the Al_2O_3 -based TECs and TCPCB-based TECs under uniform heat loading was within the listed standard deviations, implying that the two types of TECs perform equivalently under uniform heat loading. This is consistent with the two types of TECs containing the same number and size of semiconductor elements.

RESULTS UNDER CONCENTRATED HEAT LOADING

Concentrated heat loading resulted in lower efficiencies for both types of TECs. The fact that the lowest COP resulted from the Al_2O_3 -based TECs under concentrated heat loading implied that the non-uniformity of heat pumping within the TEC circuit was most severe in that case. In comparison, the COP of the TCPCB-based TECs was 87% higher than that of the Al_2O_3 -based TECs under concentrated heat loading. This reduced power consumption implied that the TCPCB had a significant heat spreading effect.

CONCLUSIONS

Concentrated heat loads on the controlled side of a thermoelectric cooler have been demonstrated to reduce the efficiency of the system in maintaining a desired temperature. The efficiency of a system with concentrated heat loads was shown to be improved when a thermoelectric cooler based on thermally conductive printed circuit boards was used instead of a traditional thermoelectric cooler based on aluminum oxide printed circuit boards.

REFERENCES

- [1] The TECs were Laird part numbers OT20,66,F0,1211 (left) and OT20,66,F0T,1211 (right).
- [2] Harvey, R. D., Walker, D. G., and Frampton, K. D., "Enhancing Performance of Thermoelectric Coolers Through the Application of Distributed Control," IEEE Transactions on Components and Packaging Technologies 30(2), 330-336 (2007).
- [3] RMT Ltd., "TEC Expert", <<http://www.rmtltd.ru/products/devices/testers/tecexpert/>> (accessed 25 March 2014)
- [4] Rowe, D. M., [Thermoelectrics Handbook: Macro to Nano], Taylor & Francis, Boca Raton, 1-6 (2006).

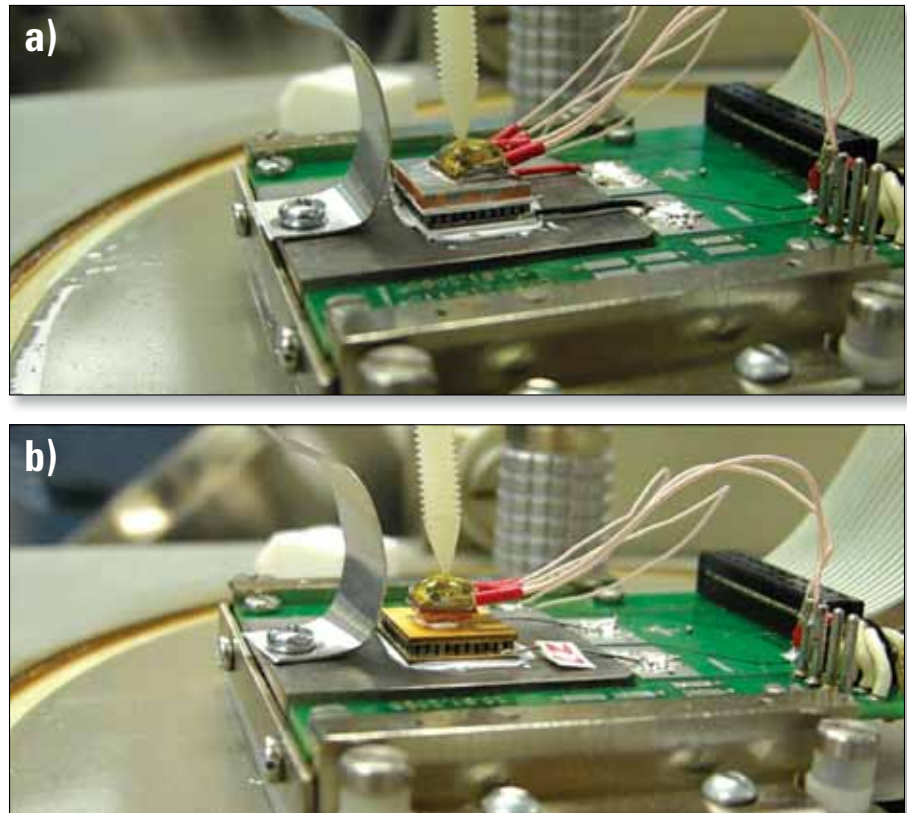


FIGURE 3: Photos of the test system with **a)** an Al_2O_3 -based TEC and large experimental heat spreader as shown schematically in Figure 2 and **b)** a TCPCB-based TEC and small experimental heat spreader installed.

TABLE 1: COMPONENT DIMENSIONS

Component	Size
Baseplate sample mounting area	30mm x 35mm
DUT [1]	11.2mm x 12.2 mm x 2.64 mm
Large experimental heat spreader	11.2mm x 12.2 mm x 1.57 mm
Small experimental heat spreader	Top 6 mm x 6 mm, bottom 3 mm x 3 mm, thickness 1.57 mm
System T_c board	6 mm x 6 mm

TABLE 2: COP VALUES

TEC under test	Experimental heat spreader contact area	Measured COP	TEC current, A	TEC voltage V
Al_2O_3 -based	3 mm x 3 mm	0.235 +/-0.014	1.36	5.58
TCPCB-based	3 mm x 3 mm	0.440 +/-0.021	0.95	4.27
Al_2O_3 -based	11.2 mm x 12.2mm	0.600 +/-0.014	0.83	3.57
TCPCB-based	11.2 mm x 12.2mm	0.577 +/-0.019	0.83	3.75

Estimating the Thermal Interaction between Multiple Side by Side Chips on a Multi-Chip Package

Je-Young Chang, Ashish Gupta
Intel Corporation

INTRODUCTION

INTEGRATION USING multi-chip packaging (MCP) is an effective and popular technology option to increase transistor density in one component by integrating two or more dice or other discrete components on a common substrate. For accurate thermal analyses of MCPs, thermal interactions between active components need to be quantified and understood. These analyses are essential, since the cooling capability of the package may be constrained by the temperature limit of an individual active device in the package.

In this article, a thermal analysis approach is presented for predicting cooling capabilities of MCP architectures. In Figure 1, an example MCP is illustrated with the locations of

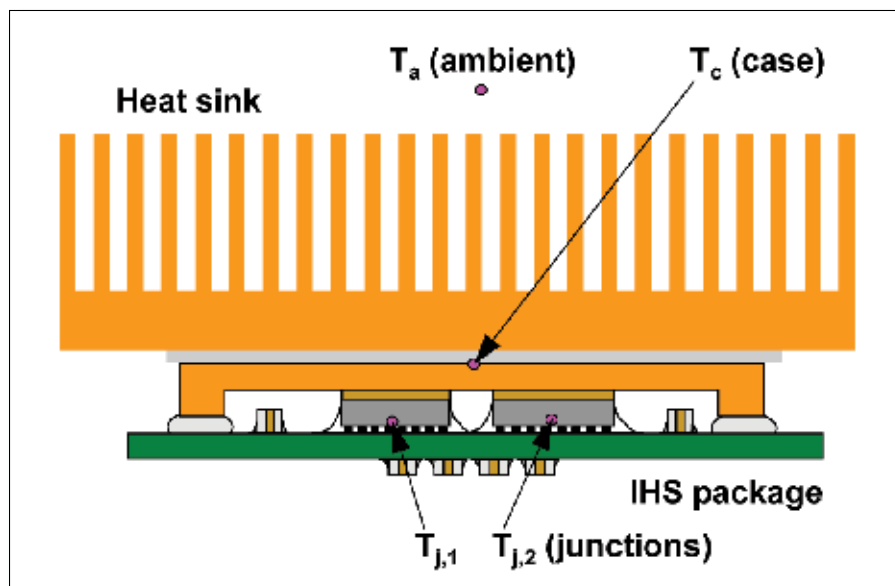


FIGURE 1: Schematic of lidded MCP with heat sink (not drawn to scale).

Je-Young Chang received his B.S. and M.S. degrees from the Seoul National University in Korea and his Ph.D. degree from University of Texas at Arlington, all in Mechanical Engineering. He worked at Penn State University for three years as a research associate before joining Intel in 2000. He has worked on many aspects of advanced cooling technologies, including two-phase immersion cooling, single/two-phase microchannel cooling, corrosion reliability of liquid cooling systems, heat pipes, TIMs, heat exchangers, etc. He has 19 issued/pending US patents, and more than 60 articles in archival journals, conference proceedings and Intel internal publications.



Ashish Gupta manages the Thermals/Fluids Core Competency Team in Intel's Assembly and Test Technology Development Group in Arizona. He holds a Ph.D. degree in Mechanical Engineering from Purdue University. His group is responsible for the R&D of advanced package thermal and cooling technologies, modeling methodologies and metrologies for Intel's current and future generations of processors for product segments during the discovery, definition, development and certification stages of technology maturity. The team's scope cover the entire gambit of Intel product segments across all market segments ranging from handheld devices and small form factor packages to higher power server products.



temperature measurements. For this example, the package has two dice under an integrated heat spreader (IHS), which is cooled by a heat sink. In this configuration, due to the proximity of the two dice, even when an adjacent die is not powered, its junction temperature will be elevated by the power applied to the other die [1-3].

For the above package, the junction temperature of any of the dice is expressed as a function of the power(s) applied to all of the dice:

$$\begin{bmatrix} T_{j,1} \\ T_{j,2} \end{bmatrix} = \begin{bmatrix} \Psi_{11} & \Psi_{12} \\ \Psi_{21} & \Psi_{21} \end{bmatrix} \cdot \begin{bmatrix} P_1 \\ P_2 \end{bmatrix} + \Psi_{ca} \cdot (P_1 + P_2) + T_a \quad (1)$$



Thermal Innovations for a Cool World

Semiconductor Thermal Measurement, Modeling and Management Symposium
T H I R T Y - F I R S T A N N U A L

CALL FOR PAPERS

March 15-19, 2015

DoubleTree Hotel, San Jose, CA, USA

The conference

SEMI-THERM is an international forum dedicated to the thermal management and characterization of electronic components and systems. It provides knowledge covering all thermal length scales from IC to facility level. The symposium fosters the exchange of knowledge between thermal engineers, professionals and leading experts from industry as well as the exchange of information on the latest academic and industrial advances in electronics thermal management. Areas of interest include, but are not limited, to the following:

Topics:

- Component, Board- and System-Level Thermal Design Approaches
- Air mover technologies with low acoustics
- Thermal Integration in the Product Design Process
- Multi-Physics Based Reliability, including Accelerated Testing
- Multi-objective design and optimization, modeling and characterization
- Novel materials: Heat Spreaders, Thermal Vias and Thermal Interface Materials
- Nanotechnology: Thermal, Mechanics, Material and Process Related Issues in Nanostructures
- Micro-Fluidics
- Characterization and Standardization of Material Property Measurements
- Energy Harvesting materials, Thermo-electrics
- Novel and Advanced Cooling Techniques/Technology,
- Roadmaps, Specifications and Traditional Cooling Limits
- Mechanical Modeling, Simulations and Characterization
- Characterization and Modeling of Multi-Scale Heat Transfer Problems
- Computational Fluid Dynamics (CFD) Analysis and Validation
- Multi-physics Modeling and Characterization of Products and Processes
- Thermal Control Methodologies

Application areas:

- Processors, ICs, and Memory
- 3-D electronics
- Wireless, Network, Computing Systems
- Data Centers
- Portable and Consumer Electronics
- Power Electronics
- Harsh Environments
- Commercial, Defense, and Aerospace Systems
- Solid-State Lighting
- Solid State Energy Generation/Cooling
- Medical and Biomedical electronics
- Instrumentation and Controls
- Micro- and nano-scale devices
- MEMS and sensors
- Alternative and Renewable Energy
- Wearables

Conference highlights

- Dedicated sessions on various application areas, novel materials, thermo-mechanical modeling/characterization techniques
- Two days of short courses (March 15 and 16, 2015), embedded tutorials and technical workshops
- Vendor exhibits: Cooling technologies, Air movers, Experimental characterization equipment and CFD simulation software

To submit an abstract

You are invited to submit an extended abstract describing the scope, contents, key results, findings and conclusions. This abstract of 2 to 5 pages is supported by figures, tables and references as appropriate. **Abstracts must demonstrate high technical quality, originality, potential impacts. Upload your abstract electronically** in RTF, DOC or PDF formats at www.semi-therm.org

Abstract Submission Deadline	Abstract Acceptance Notification	Photo-ready Full Manuscript Due
September 29, 2014	November 3, 2014	January 5, 2015

SEMI-THERM actively solicits student papers, students to co-chair sessions, and awards travel stipends and reduced conference fees.

For further information please contact the Program Chair:

Rahima Mohammed, Principal Engineer, Intel Corporation, E-mail: rahima.k.mohammed@intel.com

Visit our website: <http://www.semi-therm.org>



where $T_{j,i}$ is the junction temperature of Die “i”; P_i is the power dissipation of Die “i”; Ψ matrix, also called as “influence” coefficient matrix, is the thermal resistance from the junction to the case; Ψ_{ca} ($^{\circ}\text{C}/\text{W}$) is case-to-ambient thermal resistance; and T_a is the ambient temperature.

CALCULATION PROCESSES OF INFLUENCE COEFFICIENT MATRIX

In Equation 1, the Ψ matrix is based on the principle of linear superposition in conduction heat transfer to calculate the die junction temperatures at an arbitrary combination of powers applied to the dice under steady-state conditions. This can be extended to any number of active dice ($N \times N$ matrix) in an MCP. The above equation is also applicable to a system of multiple components with conduction being the dominant heat transfer mechanism, and provides the first order approximation of the system [1-3]. However, extra caution should be paid to systems with convection and radiation heat transfer wherein the non-linear characteristics introduced through these heat transfer modes cannot be neglected. In the above equation, Ψ_{ca} and T_a values are known at a given design condition, but $N \times N$ terms in the influence coefficient matrix must be calculated using the data collected with thermal simulations or experiments.

TABLE 1: EXAMPLE TEMPERATURE DATA FOR THE MCP PACKAGE IN FIGURE 1 ($\Psi_{ca} = 0.35^{\circ}\text{C}/\text{W}$ is assumed)

	Case 1	Case 2
Die-1 power [W]	65	55
Die-2 power [W]	17	20
$\Delta T_{j,1} = T_{j,1} - T_c [^{\circ}\text{C}]$	36.8	30.8
$\Delta T_{j,1} = T_{j,2} - T_c [^{\circ}\text{C}]$	10.9	14.1

The general calculation processes of Ψ matrix are presented below:

STEP 1: Select N different power scenarios for N active dice in the MCP. For the current example MCP shown in Figure 1, two different power scenarios, (P_1', P_2') and (P_1'', P_2''), are assumed. These power scenarios should be defined for the power ranges of interest in MCP applications. Typically, it is recommended to apply the power ranges within 10-20% of TDP value of each die in order to minimize the calculation errors due to highly non-uniform heat sources (hot spots) of the power distribution of the die, which cause non-linear spreading patterns while interacting with the power distribution of the neighboring die.

STEP 2: Calculate or measure $T_{j,i}$ values at two (N cases) different power scenarios as defined above using thermal simulations or experiments.

STEP 3: Typically, junction temperature differences from the reference point (e.g., $\Delta T_{j,i} = T_{j,i} - T_c$) are considered in actual calculations, while the downstream variables (i.e., Ψ_{ca} , T_a) are assumed constant. In this case, all the calculation results (i.e., $\Delta T_{j,i}$ and P_i values) can be summarized as:

$$\begin{bmatrix} \Delta T'_{j,1} \\ \Delta T'_{j,2} \end{bmatrix} = \begin{bmatrix} \Psi_{11} & \Psi_{12} \\ \Psi_{21} & \Psi_{22} \end{bmatrix} \cdot \begin{bmatrix} P'_1 \\ P'_2 \end{bmatrix} \text{ and } \begin{bmatrix} \Delta T''_{j,1} \\ \Delta T''_{j,2} \end{bmatrix} = \begin{bmatrix} \Psi_{11} & \Psi_{12} \\ \Psi_{21} & \Psi_{22} \end{bmatrix} \cdot \begin{bmatrix} P''_1 \\ P''_2 \end{bmatrix} \quad (2)$$

STEP 4: Rearrange the calculation results for each of $\Delta T_{j,i}$ point, which can be expressed as “power input” matrix:

$$\begin{bmatrix} \Delta T'_{j,1} \\ \Delta T'_{j,2} \end{bmatrix} = \begin{bmatrix} P'_1 & P'_2 \\ P''_1 & P''_2 \end{bmatrix} \cdot \begin{bmatrix} \Psi_{11} \\ \Psi_{12} \end{bmatrix} \text{ and } \begin{bmatrix} \Delta T''_{j,1} \\ \Delta T''_{j,2} \end{bmatrix} = \begin{bmatrix} P'_1 & P'_2 \\ P''_1 & P''_2 \end{bmatrix} \cdot \begin{bmatrix} \Psi_{21} \\ \Psi_{22} \end{bmatrix} \quad (3)$$

STEP 5: Calculate the values of the elements of the Ψ matrix using an inverse matrix solver:

**Quality Heat Sinks & Cold Plates
For Automation & Power**





OEM Supplier: Submit your design drawings here:
www.heat-sink.com.tw

Summit Heat Sinks Metal Co., Ltd.
Summit Thermal System Co., Ltd.
 Shin-lan Sec, Humen Town, Dong Guan, Tel: (86) 769-88623999
 Guang Dong, 523917 China
 E-mail: sales@summit.heat-sink.com.tw Fax: (86) 769-88623998

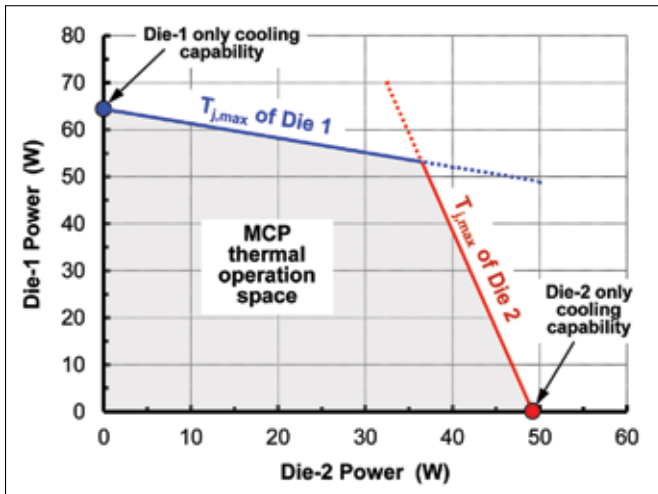


FIGURE 2. Representation of the cooling envelope of the MCP at steady-state conditions ($T_{j,max} = 100^\circ\text{C}$ for both dice and $T_a = 40^\circ\text{C}$ are assumed).

$$\begin{bmatrix} \Psi_{11} \\ \Psi_{12} \end{bmatrix} = \begin{bmatrix} P'_1 & P'_2 \\ P''_1 & P''_2 \end{bmatrix}^{-1} \cdot \begin{bmatrix} \Delta T'_{j,1} \\ \Delta T''_{j,1} \end{bmatrix} \text{ and } \begin{bmatrix} \Psi_{21} \\ \Psi_{22} \end{bmatrix} = \begin{bmatrix} P'_1 & P'_2 \\ P''_1 & P''_2 \end{bmatrix} \cdot \begin{bmatrix} \Delta T'_{j,2} \\ \Delta T''_{j,2} \end{bmatrix} \quad (4)$$

EXAMPLE CALCULATIONS

Table 1 shows example temperature data collected with thermal simulations for two different cases of die power scenarios of the MCP package in Figure 1.

For the above data, as discussed in Step 3, the temperature differences and die powers can be summarized as:

$$\begin{bmatrix} 36.8 \\ 10.9 \end{bmatrix} = \begin{bmatrix} \Psi_{11} & \Psi_{12} \\ \Psi_{21} & \Psi_{22} \end{bmatrix} \cdot \begin{bmatrix} 65 \\ 17 \end{bmatrix} \text{ and } \begin{bmatrix} 30.8 \\ 14.1 \end{bmatrix} = \begin{bmatrix} \Psi_{11} & \Psi_{12} \\ \Psi_{21} & \Psi_{22} \end{bmatrix} \cdot \begin{bmatrix} 55 \\ 20 \end{bmatrix} \quad (5)$$

The above equations can be rearranged for each of $\Delta T_{j,1}$ and $\Delta T_{j,2}$ values, as discussed in Step 4, and “power input” matrix can be expressed as:

$$\begin{bmatrix} 36.8 \\ 30.8 \end{bmatrix} = \begin{bmatrix} 65 & 17 \\ 55 & 20 \end{bmatrix} \cdot \begin{bmatrix} \Psi_{11} \\ \Psi_{12} \end{bmatrix} \text{ and } \begin{bmatrix} 10.9 \\ 14.1 \end{bmatrix} = \begin{bmatrix} 65 & 17 \\ 55 & 20 \end{bmatrix} \cdot \begin{bmatrix} \Psi_{21} \\ \Psi_{22} \end{bmatrix} \quad (6)$$

In the above equations, the values of Ψ matrix elements can be calculated from an inverse matrix solver, and the complete form of Equation 1 for the MCP package in Figure 1 can be written as:

$$\begin{bmatrix} \Delta T_{j,1} \\ \Delta T_{j,2} \end{bmatrix} = \begin{bmatrix} 0.582 & -0.060 \\ -0.059 & 0.868 \end{bmatrix} \cdot \begin{bmatrix} P_1 \\ P_2 \end{bmatrix} + 0.35 (P_1 + P_2) + T_a \quad (7)$$

GRAPHICAL REPRESENTATION OF MCP COOLING ENVELOPES

In Equation 7, there are two linear equations expressed in terms of P_1 and P_2 :

$$\begin{aligned} 0.932P_1 + 0.290P_2 &= T_{j,1} - T_a \\ 0.291P_1 + 1.22P_2 &= T_{j,2} - T_a \end{aligned} \quad (8)$$

The above two linear equations can be used to represent cooling capabilities of Die 1 and Die 2 as defined by junction temperature limits and ambient temperature condition. In Figure 2, cooling capability curves of two dice in the MCP in Figure 1 are illustrated. As shown, the solid lines represent the cooling capabilities of Die 1 and Die 2 with respect to junction temperature limits and ambient temperature condition, and the overlapped region (highlighted with gray color) represents thermal operation space of the MCP.

The above graphical representation of the cooling envelope of the MCP is useful to estimate thermal operation spaces for different design conditions, such as different junction temperature limits, ambient temperatures and heat sink designs. It should be noted that, for accurate estimation of thermal operation space, the Ψ matrix should be re-calculated, if there is any significant change in:

- Design conditions, such as die dimensions, die locations, die-to-die spacing, IHS dimensions, etc.
- Material conductivities, such as thermal interface conductivity.
- Die non-uniform heating powermaps.

REFERENCES

- [1] Lall, B., Guenin, B., and Molnar, R., “Methodology for Thermal Evaluation of Multichip Modules,” IEEE Trans. CPMT, Vol. 18, No. 4, pp. 758-764, 1995.
- [2] Zahn, B., “Steady State Thermal Characterization of Multiple Output Devices Using Linear Superposition Theory and a Non-Linear Matrix Multiplier,” Proceedings of 14th SEMI-THERM Conference, pp. 39-46, 1998.
- [3] Guenin, B., “So many Chips, So Little Time; Device Temperature Prediction in Multi-Chip Packages,” Electronics Cooling, Vol. 12, No. 3, August 2006.



Kunze Folien GmbH

Raiffeisenallee 12a
82041 Oberhaching, Germany
Phone: +49 89 666682-0
Fax: +49 89 666682-10
sales@heatmanagement.com
www.heatmanagement.com

Gap Pads & Fillers Heat Sinks Heat Spreaders
Interface Materials Liquid Cooling Phase Change Materials
Thermal Tapes Thermally Conductive Graphite Films

Solder Joint Lifetime of Rapidly Cycled LED Components

Ir. G. A. (Wendy) Luiten
Philips Research

INTRODUCTION

ACTIVE LEDs in a consumer TV product are boosted and dimmed with the video picture content. Boosting and dimming of LEDs is a powerful means to improve visual experience, either through application of active LEDs in an ambient light feature, or through dimming and boosting of the display LEDs in a direct lit video display. Active driving of LEDs is also a significant consideration in the thermal management of a video display product [1, 2]. However, active driving of LEDs increases the number of temperature cycles by several orders of magnitude, and thermal cycling is well known to lead to so-called low cycle fatigue solder joint failure. How then will active driving of LEDs affect the lifetime of LED solder joints in a TV product?

SOLDER FATIGUE AT LONG TIME SCALE

The root cause of low cycle fatigue

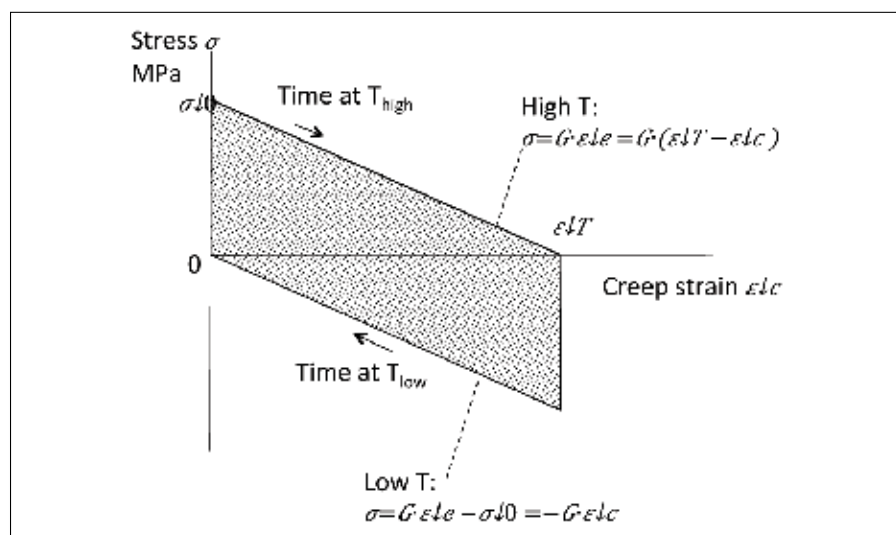


FIGURE 1: Stress-creep strain loop from cyclic thermal load.

solder joint failure is that thermal mismatch between a component and PCB is taken up in deformation of the solder joint. Assume that a SMD LED is subjected to an instantaneous temperature rise ΔT at $t=0$ s. This

results in a thermal shear strain ϵ_T in the solder joint, proportional to the temperature change, $\epsilon_T \sim \Delta T$. At $t=0$ s, the entire thermal strain is taken elastically. By Hooke's law, the shear stress σ is proportional to the elastic strain ϵ_e with proportionality constant G , the solder's shear modulus $G = \frac{E}{2(1+\nu)}$. Thus, at the instantaneous temperature rise $\sigma_0 = G \cdot \epsilon_e = G \cdot \epsilon_T$. At longer times the solder starts to creep, that is, to flow very slowly, and part of the thermal strain is taken in creep strain ϵ_c . This lowers the elastic strain and the stress relaxes.

$$\sigma = G \cdot \epsilon_e = G \cdot (\epsilon_T - \epsilon_c) \quad (1)$$

When the creep strain equals the thermal strain, $\epsilon_c = \epsilon_T$, the elastic

Wendy Luiten is a senior thermal specialist at Philips Research in Eindhoven. She has 25+ years experience in the thermal and mechanical fields and 15+ years experience in cooling consumer electronics products. She is also a lecturer at electronics cooling and thermal design workshops, presently through the High Tech Institute Eindhoven, and has lectured 25+ times in Asia, the Middle East, the US and Europe. She is the lead author on numerous papers, and holds 4 patents. Luiten received the best paper award at Semi-Therm 2002 and the Harvey Rosten award for Excellence 2013, and is a member of the Thermic steering committee and Semi-Therm and Thermic program committees. Wendy Luiten received a MSc in mechanical engineering (heat & fluid flow) from Twente Technical University in the Netherlands.



strain is zero and the joint is stress-free. If the temperature is then lowered by $-\Delta T$, the change of temperature with respect to the stress-free situation will again cause a thermal mismatch, which will again cause stress in the solder joint, $-\sigma_0$, which will again relax away to the stress-free situation through solder creep. In this manner, temperature cycles result in cyclic loading, creep and stress relaxation in the solder joint. The diagram of stress versus creep strain is shown in Figure 1.

In each cycle, an amount of damage is incurred that is proportional to the area inside the stress-creep strain loop. Solder joint failure occurs once the total accumulated creep damage exceeds a certain value C , which is usually determined through an accelerated test. Figure 1 shows that the area inside the loop for a full creep cycle up to the stress free situation equals $\sigma_0 \cdot \epsilon_T$. It follows that the area of the loop is proportional to ΔT^2 :

$$\text{Area} = \sigma_0 \cdot \epsilon_T = G \cdot \epsilon_T^2 \sim \Delta T^2 \quad (2)$$

A similar relationship is also found in the low-cycle fatigue law of Coffin-Manson [4], in the work of Engelmaier [5, 6] and of Norris-Landzberg [10] in the form of fatigue exponent, which roughly corresponds to a value 2. The quadratic dependency is also the basis for the common design rule relating the number of cycles to failure in operation N_f to the number of cycles to failure N_{test} in an accelerated test with temperature sweep ΔT_{test} :

$$N_f = \frac{N_{test} (\Delta T_{test})^2}{\Delta T^2} \quad (3)$$

The fatigue cycle shown in Figure 1 will only appear if the heating and cooling is instantaneous, and if dwell times are sufficiently long to allow for relaxation up to the stress free situation. It is well-known that the durations of ramp time and dwell time have a significant impact in accelerated temperature cycle tests [7]. Both the Engelmaier and the Norris-Landzberg model incorporate the effect of field vs. test timing in a time factor in their models. However, it is not obvious that these models are appropriate for short video time cycles. Typical temperature cycle tests have at most one order of magnitude difference from test to field condition. Since temperature effects dominate the acceleration factors, it then becomes difficult to separate out time effects with accuracy. Furthermore lifetime, test timing parameters and test temperatures are interrelated in a complex manner [10]; therefore, separation of time and temperature effects does not lend itself to extrapolating with confidence. As an example, the Engelmaier relations were critically reviewed in [8] and shown not to be reliable for several cases. Hence using existing simple models incorporating the cycle time effects is not straightforward for short video cycles and more accurate numerical investigation using FEM are often not possible in view of limited project resources.

TABLE 1: SAC MATERIAL PROPERTIES

parameter	value	unit
Schubert model		
A	277984	s^{-1}
B	0.02447	MPa^{-1}
C	6.41	
D	6500	K^{-1}
Elastic constants		
E	61251 - 58.5 T	MPa, T in Kelvin
v	0.36	

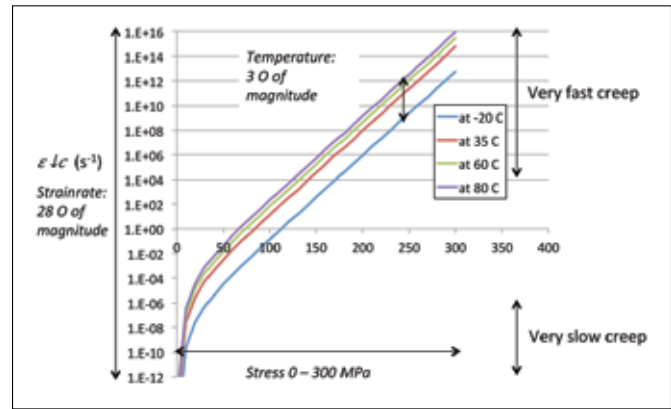


FIGURE 2: Creep strain rate $\epsilon \downarrow c$ (s^{-1}) as a function of stress σ (MPa).

SOLDER FATIGUE AT SHORT TIME SCALE

The purpose of the current work is to find out the influence of short cycle times on solder failure in a less resource-intensive manner, allowing for a better lifetime estimate in a safe engineering envelope. Direct integration of the creep strain rate is used to determine how much creep will actually occur in the cycle time.

The flow rate or creep strain rate of solder is extremely dependant on stress and temperature. According to Syed's formulation of the Schubert model for lead-free solder [9], the creep strain rate is the product of a stress dependent part $g(\sigma)$ and a temperature dependent part $f(T)$.

$$g(\sigma) = A \{\sinh(B\sigma)\}^C \quad (4)$$

$$f(T) = \exp\left(\frac{D}{T}\right) \quad (5)$$

$$\dot{\epsilon}_c = g(\sigma)f(T) = A \{\sinh(B\sigma)\}^C \exp\left(\frac{D}{T}\right) \quad (6)$$

Table 1 shows the values for the material parameters A through D, as well as the elastic modulus E and Poisson ratio ν .

Figure 2 shows the calculated creep strain rates for a -20 °C to 85 °C temperature range and 0 – 300 Pa stress range.

It shows that the shear strain rate varies 28 orders of magnitude over the stress range. At high stress levels, the extremely high creep strain rate will immediately relax the stress to a lower level, so this part of the stress relaxation does not cost significant time. At low stresses, the very low creep rate will result in negligible creep in the time range of $1 - 10^4$ s. Figure 2 also shows that the creep strain rate varies three orders of magnitude in the temperature range -20°C to $+80^\circ\text{C}$. In contrast, from Table 1, the variation in the elastic modulus over the same temperature range is only 14%. Therefore, in all subsequent calculations the shear modulus will be taken at the mean temperature of the high and the low temperature.

Total creep in the cycle time is closely coupled to the amount of stress relaxation. The stress relaxation curves at a certain temperature are obtained in the following way:

The shear stress is proportional to the shear strain. Taking the time derivative of Equation 1 and substituting Equation 6:

$$\dot{\sigma} = -G\dot{\epsilon}_c = -G \cdot g(\sigma)f(T) \quad (7)$$

For sufficiently small increments $\Delta\sigma$, this can be used to find the time that it takes to realize the stress increment.

$$\Delta t = \frac{\Delta\sigma}{\dot{\sigma}} \quad (8)$$

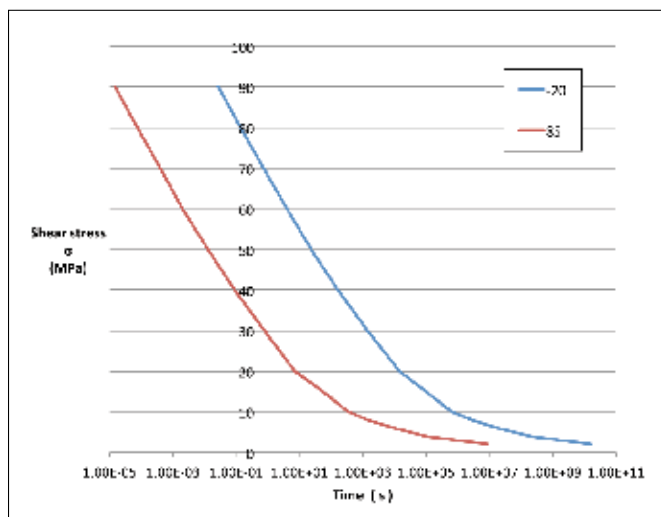


FIGURE 4: Stress relaxation curves at -20°C and $+85^\circ\text{C}$.

$\epsilon \downarrow c(\sigma)$ from Schubert model

$$\sigma = G \cdot \epsilon \downarrow c = G \cdot (\epsilon \downarrow T - \epsilon \downarrow c)$$

$$\sigma = -G \epsilon \downarrow c$$

$$dt = \Delta\sigma / \dot{\sigma}$$

$$t = \sum dt$$

$$\sigma(t)$$

T [°C]	20	85
T [K]	293	358
G [Pa]	7979	7979
strainrate "part"	6.55403E-12	1.3026E-06
shearstress	stress rate	c
MPa	MPa/s	s
152	8.17E-05	2.69E-06
133	2.57E-05	3.09E-06
123	5.32E-06	1.88E-06
113	1.0E-06	9.13E-07
103	2.24E-08	4.46E-08
90	4.33E-02	2.21E-02
80	8.57E-02	1.11E-02
70	1.72E-01	5.61E-03
60	3.4E-01	2.70E-03
50	5.17E-01	1.33E-03
40	7.25E-02	1.38E-02
30	7.48E-02	1.34E-03
20	4.07E-04	1.23E-04
15	1.77E-06	5.67E-06
10	3.9E-08	5.65E-08
8	9.26E-09	2.6E-06
6	1.44E-07	1.39E-07
4	1.06E-08	1.89E-08
2	1.22E-10	1.67E-10

FIGURE 3: Spreadsheet implementation.

Summing the time increments associated with the stress increments results in an approximation of the stress relaxation over time. The whole scheme is easily implemented in a spreadsheet, as shown in Figure 3. The corresponding stress relaxation curves at -20°C and $+85^\circ\text{C}$ are shown in Figure 4.

Similar curves can be made for different initial stress levels and different temperatures, and these are used to determine how much stress relaxation will take place in a certain creep time. Subsequently the stress-creep strain cycle can be constructed.

VIDEO LED APPLICATION

We consider an idealized temperature cycle with instantaneous temperature change and an equal time at the high and at the low temperature. Four cases are of interest: a) the accelerated test, b) the on/off cycle, c) a long 100 s video cycle, and d) a short 5 s video cycle. Figure 5 shows the calculated stress/creep strain cycles and Table 2 the load case details and resulting creep strain.

In all cases, even in the accelerated test, creep times turn out to be too short for full creep to occur. Figure 5 and Table 2 show that using a large temperature step in the accelerated test case works out like intended: the area of the test cycle is much larger compared to the use cycles, thus failure will be accelerated and the failure energy value can be obtained in shorter time. Creep in the on/off cycle case is slightly less complete compared to the accelerated case, therefore using the accelerated test to predict the number of cycles to failure as per the normal design rule in Equation 3 works out well with a sensible engineering margin of $(79/71-1)=11\%$. This is not the case for the video cycles. Not taking the short time effect into account leads to roughly a factor 2 underestimation in lifetime for the long video cycle. In case of the short video

TABLE 2: LOAD CASES

		T_{low}	T_{high}	creep time	ΔT	ε_T	σ_0	% full creep
	case	C	C	s	C		MPa	
a	Accelerated test	-20	85	3000	105	0.95%	152	79%
b	on/off	35	80	3600	45	0.41%	63	71%
c	long boost	60	90	100	30	0.27%	41	37%
d	short boost	60	80	5	20	0.18%	27	0%

cycle, the temperature excursions are all taken elastically, no creep damage is incurred and use of Equation 3 is not appropriate at all. This shows that for short cycle times the time effect must be taken into account for correct lifetime prediction of the solder joints.

SUMMARY AND CONCLUSION

The effect of short creep time on low cycle fatigue failure of SMD LEDs was investigated. It was shown that for an idealized case with instantaneous temperature change, full creep i.e. stress relaxation to the stress free level and with temperature independent elastic moduli, the creep damage per cycle is proportional to ΔT^2 . Direct integration was used to construct stress relaxation curves incorporating the highly non-linear behavior of the lead free solder as per the Syed/Schubert model; these were used to construct a simplified stress-strain fatigue cycle, incorporating the effect of creep time. Application to active LEDs in a TV product demonstrated the validity of accelerated testing and the ΔT^2 design rule to product on/off cycles. In contrast, this was not the case for the typical video cycle times. The short cycle times only allow for partial creep, doing less damage per cycle, and so the use of the uncorrected design rule leads to under prediction of solder joint lifetime. At very short cycle times, the cyclic thermal mismatch is taken fully in elastic excursions with no creep at all, and low cycle fatigue is not the appropriate failure mode. Although the complexity of the solder joint fatigue cycle was very much simplified in the work, the approach was shown to be of merit in clarifying main effects in low cycle solder fatigue, and in enabling correct first order engineering estimations using only a commercial spreadsheet.

ACKNOWLEDGMENTS

The support of Philips Research and of TP Vision Innovation sites Eindhoven and Bruges is gratefully acknowledged.

REFERENCES

[1] Luiten, G. A., Chapter 14, "Thermal Challenges in LED-Driven Display Technologies: State-of-the-Art" in C. J. M. Lasance, A. Poppe (eds.), Thermal Management for LED Applications, 1 Solid State Lighting Technology and Application Series 2, DOI 10.1007/978-1-4614-5091-7_14, July 2013

[2] Luiten, G. A. and ter Weeme, B. J. W. (2011), "Thermal management of LED-LCD TV display", Journal of the Society for Information Display, 19: 931–942. doi: 10.1889/JSID19.12.931

[3] van Driel WD, Yuan CA, Koh S, Zhang GQ (2011) "LED system reliability", 12th. Int. Conf. on Thermal, mechanical and multi-physics simulation and experiments in microelectronics and microsystems EuroSimE 2011, pp 1/5–5/5

[4] [http://en.wikipedia.org/wiki/Fatigue_\(material\)](http://en.wikipedia.org/wiki/Fatigue_(material)), last retrieved 15 June 2013

[5] Engelmaier, W., "Achieving Solder Joint Reliability in A Lead-Free World, Part 1", Global SMT & Packaging, Vol. 3, No.6, June 2007, pp. 40-42

[6] Engelmaier, W., "Achieving Solder Joint Reliability in A Lead-Free World, Part 2", Global SMT & Packaging, Vol. 7, No.8, August 2007, pp. 44-46

[7] Y. S. Chan and S. W. Ricky Lee, "Detailed Investigation on the Creep Damage Accumulation of Lead-free Solder Joints under Accelerated Temperature Cycling "11th. Int. Conf. on Thermal, Mechanical and Multiphysics Simulation and Experiments in Micro-Electronics and Micro-Systems, EuroSimE 2010

[8] Preeti Chauhan, Michael Osterman, S. W. Ricky Lee, and Michael Pecht, "Critical Review of the Engelmaier Model for Solder Joint Creep Fatigue Reliability" IEEE Transactions On Components And Packaging Technologies, Vol. 32, No. 3, September 2009

[9] Ahmer Syed, "Accumulated Creep Strain and Energy Density Based Thermal Fatigue Life Prediction Models for SnAgCu Solder Joints", originally published 54rd ECTC 2004, (pp 737 – 746), corrected version retrieved 06052010 http://ansys.net/ansys/papers/asyed_ectc2004_corrected.pdf

[10] Michael Osterman, "Effect of Temperature Cycling Parameters (Dwell and Mean Temperature) on the durability of lead-free solders" IMAPS Chesapeake Area Winter symposium Jan. 27, 2010

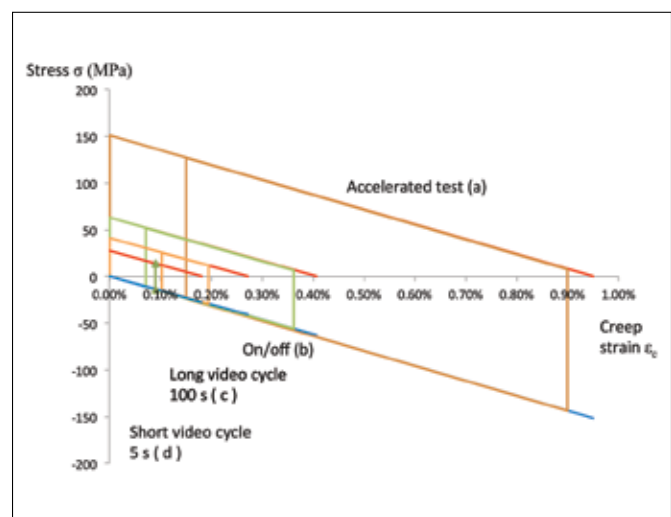


FIGURE 5: Stress – creep strain loops.

Challenges in Measuring Theta jc for High Thermal Performance Packages

Jesse Galloway, Ted Okpe
Amkor Technology

ONE OF THE MORE challenging thermal resistance measurements to make for electronic packages is the junction-to-case resistance called Theta jc. The equation for Theta jc, Equation 1, is straightforward. However, the difficulty lies in making an accurate case temperature, T_c , without affecting the junction temperature, T_j , and the flow of heat, P_{th} , into the cold plate.

$$\Theta_{jc} = \frac{(T_{j,max} - T_c)}{P_{th}} \quad (1)$$

For uniform power distribution, Theta jc is calculated by taking the difference between the junction and the case temperature, all measured at the center of the package, divided by the power flowing into the cold plate. In reality, the case temperature cannot be measured without disturbing the heat

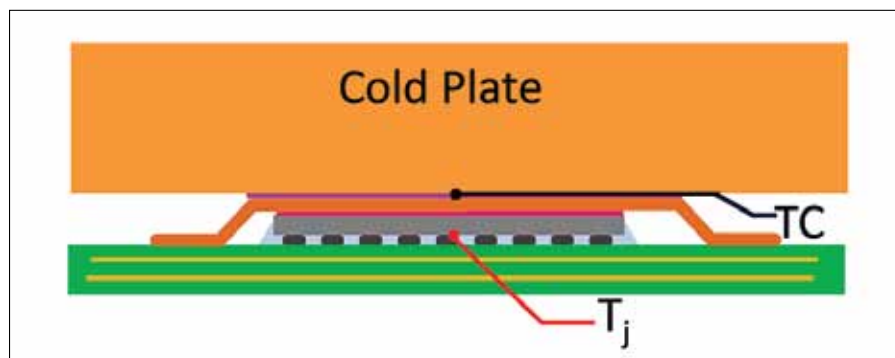


FIGURE 1: Theoretical method for measuring Theta jc.

flow once a sensor is inserted between the case and the cold plate as shown in Figure 1.

This shortcoming may be resolved for packages that have a predominate heat flow path. For example, heat flows at least 90% from the die to the copper slug in an exposed pad thin quad flat pack (eTQFP) package. A transient

method was proposed by [1] as a means for measuring Theta jc without having to measure the case temperature. A JEDEC standard, JESD51-14 [2], summarizes the method for measuring Theta jc using a transient method. For packages such as a plastic ball grid array (PBGA) and flip chip ball grid array (FCBGA) packages, heat flow is multidirectional. Hence a direct application of the transient standard [2] may not be appropriate.

The JEDEC JC-15 thermal standards committee has devoted a considerable amount of time discussing ways to overcome difficulties in making steady-state Theta jc measurements. At this time it has not reached a consensus for writing a standard. The purpose of this study was not to propose a steady-state Theta jc standard but to document how the design of the cold plate and case temperature sensor affects Theta jc measurements and to make general recommendations on the benefits of one method compare to another.

Experimental measurements were

Jesse Galloway, Ph.D., supports thermal characterization of current package technologies while investigating opportunities for enhancing new packaging concepts. His technical interests include testing thermal interface materials and automating thermal analyses. Jesse has over 25 years of experience in electronic cooling. Jesse has published over 30 articles in archival journals and conference proceedings.





Ted Okpe graduated from Arizona State University in 2013 with a bachelor's degree in mechanical engineering. He works at Amkor's A4 lab in Chandler, Arizona supporting thermal characterization of thermal interface materials. Ted's technical interests include design testing hardware and developing data acquisition systems.



made using a 23mm x 23mm body plastic ball grid array (PBGA) package. Four different samples were tested, P1, P2, P3 and P4. A 40mm flip chip ball grid array (FCBGA) package was also tested using four different samples, F2, F3, F4 and F5. A summary of the package dimensions are given in Table 1. Both packages were fabricated using thermal die equipped with heaters. A uniform power distribution was applied to the active surface of the die. Each die had a temperature sensor located at its center. The PBGA package had a mold cap thickness of 1.17mm with a die thickness of 0.3mm. The FCBGA package was constructed using a single piece copper lid with a 1.0mm thickness. Approximately 100W was applied to the FCBGA while approximately 8W was applied to the PBGA package. The measured Theta jc differed by as much as 300% depending on which method was used to measure the case temperature.

Four different cold plate designs were developed to measure Theta jc. In all cases, the same water-cooled cold plate design was used to remove heat from the devices under test. The

TABLE 1: PACKAGE DESCRIPTION

	PBGA	FCBGA
Image		
Body (mm)	23 x 23	40 x 40
Die (mm)	10.2 x 10.2	15.6 x 14.8
Power (W)	8	100
Theta jc (C/W)	0.8 - 3.0	0.06 - 0.20

first design used a spring loaded thermocouple (36 gauge type K) positioned normal to the surface of the package inserted directly through the cold plate in between cooling channels. A spring was used to create a compressive force, driving the thermocouple bead against the case surface with a force of approximately 1.5N. The second design used an embedded thermocouple (36 gauge type K) mounted parallel to the surface of the package inside a 5mm thick copper reference plate. This reference plate made contact to the same cold plate design

Don't miss out on the industry's premier event!

The only event
that encompasses
the diverse world
of integrated
systems packaging!



May 27-30, 2014

**The Walt Disney World
Swan & Dolphin Resort**

**Lake Buena Vista
Florida, USA**

For more
information, visit:
www.ectc.net



**The 64th Electronic Components
and Technology Conference**

**MORE THAN 300
TECHNICAL PAPERS COVERING:**

- 3D/TSV
- Advanced Packaging
- Modeling & Simulation
- Optoelectronics
- Interconnections
- Materials & Processing
- Applied Reliability
- Assembly & Manufacturing Technology
- Electronic Components & RF
- Emerging Technologies

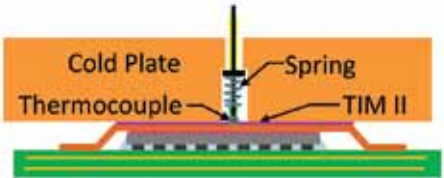
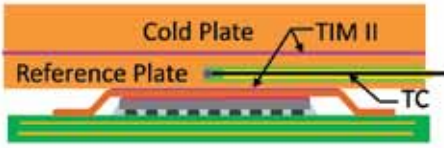
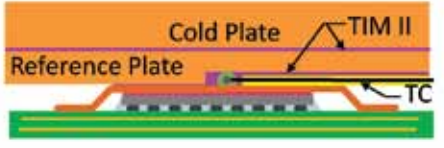
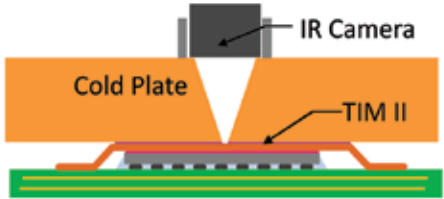
Conference Sponsors:




HIGHLIGHTS

- 41 Technical Sessions including:
 - 5 Interactive Presentation Sessions, including one featuring student presenters
- 18 CEU-approved Professional Development Courses
- Technology Corner Exhibits, featuring more than 95 industry-leading vendors
- 5 Special Invited Sessions
- Several evening receptions
- Wednesday luncheon keynote speaker
 - Peter L. Bocko, CTO, Corning Glass Technologies
- Multiple opportunities for networking
- Great location

TABLE 2: COMPARISON OF THE THETA JC COLD PLATE DESIGN AND CASE TEMPERATURE MEASUREMENTS

Temperature Sensor	Cold plate design	Effect on case temperature	Effect on junction Temperature
Contact TC		Temperature gradient through TIM had a small effect on case temperature.	Has small effect at high power
Embedded TC		Does not read case temperature accurately. Large errors for high power tests	Large impact at high power
Glued TC		Temperature gradient through TIM affects measurements. Difficult to make reliable TC contact with the case.	Large impact at high power
Optical		May affect case temperature for low conductivity packaging materials. Heat flow is affected by hole in cold plate.	Has small effect at high power

that was used for the contact thermocouple test. A 1.5mm hole was drilled in the center of the reference plate and filled with silver epoxy. Then, the thermocouple was inserted to the end of the hole and the epoxy was cured. The third design glued the thermocouple bead to the case surface at its center using silver filled epoxy. A 1.5mm wide x 1.0mm deep groove was machined into the surface of the 5mm copper reference plate to provide an escape path for the thermocouple leads. Again, the same cold plate was used to remove heat from the device under test. The fourth design used a fine focus infrared camera having a spot size of 1mm. The cold plate was modified to create a cone-shaped optical access port to view the surface. A 2.0 mm hole was exposed at the cold plate surface and extends backward at a 35 degree cone angle. For all methods, the thermocouples and IR camera were calibrated against a known standard over a temperature range from 30C to 50C. Each method had relative merits and drawbacks as outlined in Table 2.

The temperature rise between the die and the case were plotted in Figure 2a for the FCBGA packages and Figure 2b for the PBGA packages. The contact and optical methods had a similar junction-to-case temperature difference. In comparison, the glued and the embedded thermocouple

junction-to-case temperature differences were larger. Epoxy covered the glued thermocouple bead with an effective bead diameter of approximately 0.4mm. It senses not only the case temperature but also the TIM II temperature. There was more part-to-part variation in temperature difference for the glued thermocouple method compared to other methods. The embedded thermocouple is isolated from the case by a TIM II layer. As a consequence, the glued thermocouple and the embedded thermocouple measured case temperatures will be lower than the actual case temperature, yielding a greater junction-to-case temperature difference.

The optical cold plate design, with a larger hole in the center, affects the conduction flow path to a greater extent compared to the other cold plate designs. Heat flowing from the die to the case center location must spread laterally. For the PBGA package, the case temperature is artificially raised as a consequence since heat does not spread as efficiently through the lower conductivity mold compound ($k \sim 1.0\text{W/m/k}$). The corresponding junction-to-case temperature difference was smaller for the PBGA package tested using the optical cold plate. The glued and the contact thermocouple gave similar temperature differences. At the smaller power level applied to the PBGA packages, the temperature gradient through the

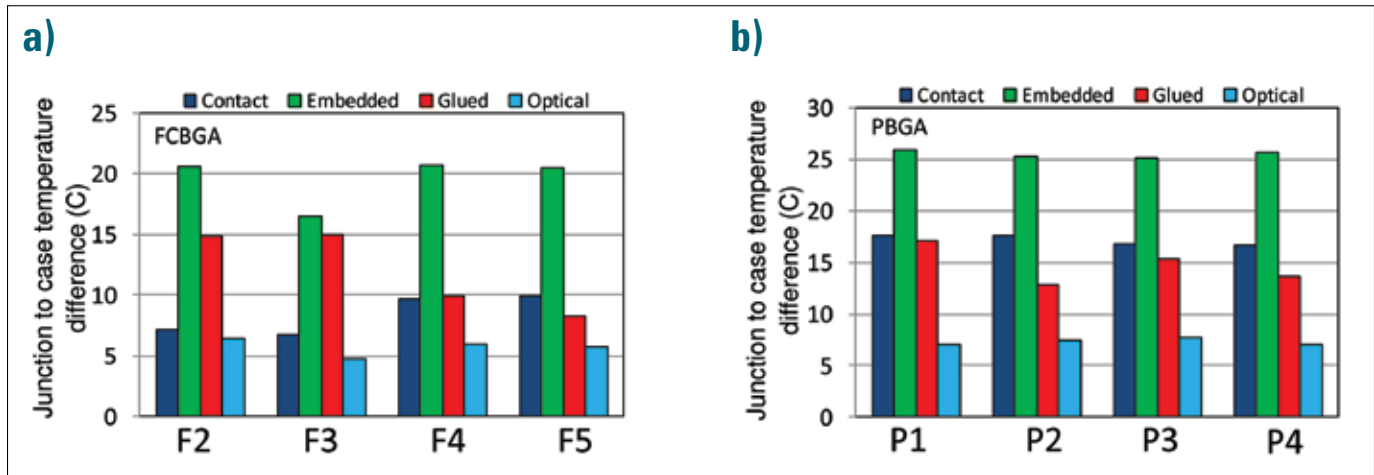


FIGURE 2: a) Temperature difference between the junction and case for FCBGA packages F2, F3, F4 and F5 b) for PBGA packages P1, P2, P3, and P4.

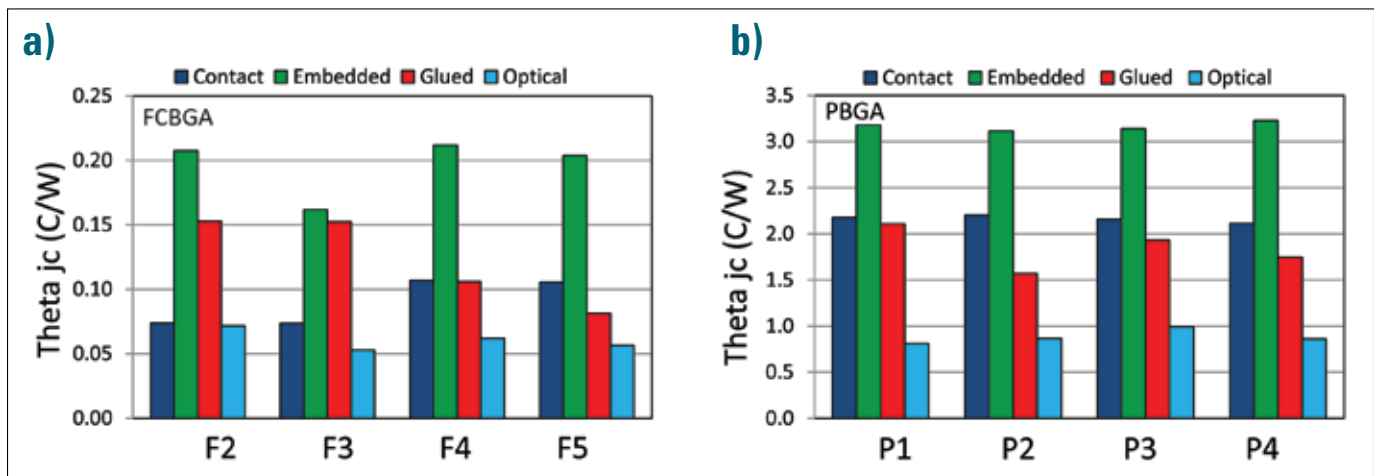


FIGURE 3: a) Theta jc for FCBGA package as a function of package size and test method. b) Theta jc for PBGA package as a function of package size and test method.

TIM II layer was smaller, hence the glued thermocouple error was also smaller. Just as was observed for the FCBGA package, the embedded thermocouple design gave the highest temperature difference for the PBGA package due to the extra TIM II layer separating the sense location and the actual case surface.

Using temperature data reported in Figures 2a and 2b and power data, the measured Theta jc data were calculated using equation 1 and plotted in Figure 3. There was a considerable difference in the Theta jc data depending on which method was employed. The highest Theta jc values were recorded for the embedded TC method and the lowest with the optical method. The optical and contact methods gave similar results for the FCBGA package. The contact and the glued thermocouple gave similar results for the PBGA package.

In order to determine which method provided the more accurate case temperature measurement, a calibration standard was developed to measure errors in reading the surface temperature. The calibration standard consisted of a calorimeter bar instrumented with five thermocouples, equally spaced at

2.5mm intervals along the center line of the bar, see Figures 4a and 4b. Note that two thermocouples are visible in Figure 4a. There are three more thermocouples mounted on the opposite side that are not visible in this picture. Two cartridge heaters supplied power to the base of the standard. The FCBGA case temperature standard was machined from oxygen free copper, thermal conductivity of 395W/m/k, to enable higher power testing. The PBGA case temperature standard was machined from hastelloy, a low thermal conductivity material (10W/m/k). It enabled greater temperature difference to be read at a lower power level that was used to test PBGA packages.

The case temperature was determined by extrapolating the temperature gradient to the upper surface. The linearity of temperature versus thermocouple position was quite good resulting in an R^2 fit typically greater than 0.999. Each individual case temperature method was compared to the standard value using a setup shown in Figure 4b. The standard was tested following the same method that was used to test the PBGA and FCBGA packages. The case temperature error

was calculated as the difference between the extrapolated surface temperature and the measured case temperature. The temperature error was plotted in Figure 5 as a function of the applied power. Greater corrections are required for the embedded thermocouple method compared to the other methods. The optical method required the least amount of correction for high power packages and the contact method required the least amount of correction for lower power packages.

Generally speaking, methods that required large temperature corrections created greater uncertainty in the final Θ_{jc} measurement. Therefore, both the embedded and the glued thermocouple methods should be avoided in measuring Θ_{jc} . The embedded method was dependent on the TIM II thermal resistance. The glued thermocouple method was dependent on the type of epoxy used to glue it to the case and the skill of the technician in attaching it. Both the contact thermocouple method and the optical method require additional investigation to determine which method is preferable. had several advantages including lower cost and more readily available. It also did not require a larger hole in the center of the heat sink as was required for the optical method. The optical method had the advantage of providing a true case temperature measurement. Additional work is planned using finite element analysis to understand the interaction between the temperature sensor and the case surface including the effects of the cold plate design.

CONCLUSIONS

- Θ_{jc} data was dependent on the cold plate design and the temperature sensor used to measure the case temperature.
- Θ_{jc} data for PBGA and FCBGA packages may vary by more than 300% depending on the cold plate design and temperature sensor.
- A calibration standard was presented as a means for

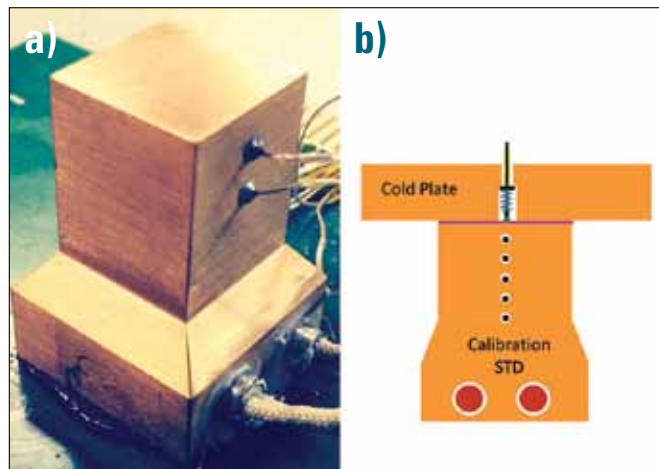


FIGURE 4. a) Calibration standard. b) Calibration standard being used to test the contact thermocouple cold plate.

determining which method provided the more accurate case temperature.

- The optical and contact case temperature methods require less case temperature correction.
- The optical and contact case methods should be explored further to understand which method provides the more reliable and accurate case temperature measurement with less impact on the heat flow from the package.

REFERENCES

- [1] D. Schweitzer, "Transient Dual Interface Measurement of the R_{th-JC} of Power Semiconductor Packages", *ElectronicsCooling*, Vol. 16, No. 3, 2010.
- [2] JEDEC Standard JESD51-14, "Transient dual interface test method for the measurement of the thermal resistance junction-to-case of semiconductor devices with heat flow through single path", November 2010, <http://www.jedec.org/standards-documents/results/JESD51-14>.

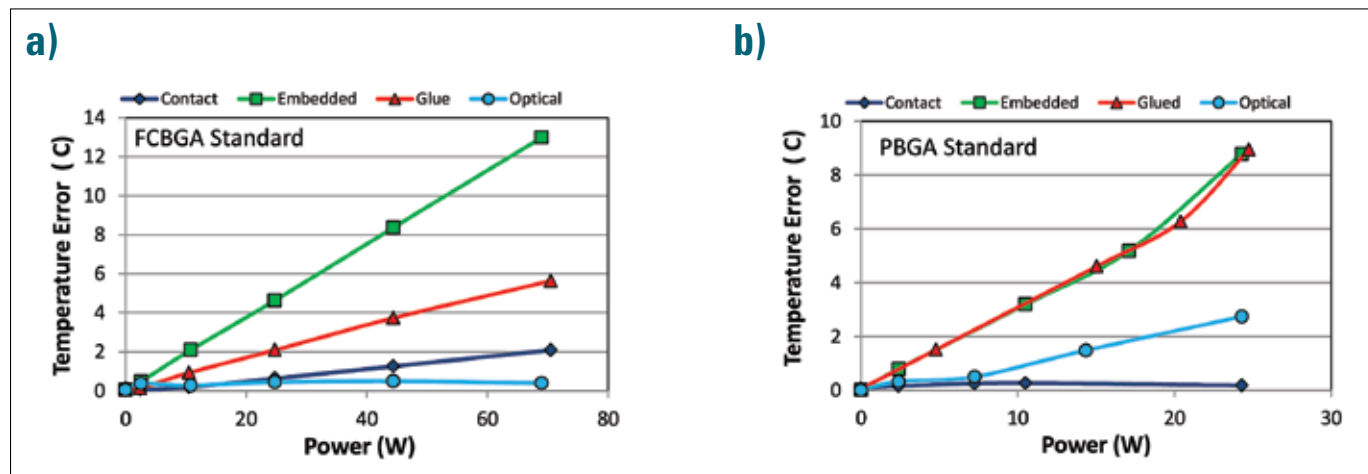


FIGURE 5: Temperature error between calibration standard and case temperature measurement. **a)** High power package testing calibrated using a standard made from copper (thermal conductivity of approximately 395W/m.k). **b)** Lower power packages tested using a standard made from hastelloy (thermal conductivity of approximately 10W/m.k).

**20th International Workshop on
Thermal Investigations of IC's and Systems
Greenwich, London, UK**

24th - 26th Sept, 2014

Register Online

*Detailed information about
the agenda and workshops:*

www.therminic2014.eu



Commercial sponsor:

**Mentor
Graphics®**

— Mechanical Analysis

THERMINIC 2014

Advances in Vapor Compression Electronics Cooling

James Burnett
Aspen Systems

INTRODUCTION

OVER THE LAST 10 years, there has been a well documented increase in the energy density of electronic devices. As this energy density has gone up, so has the heat dissipation on electronics packages. In response to this challenge, significant research has taken place to develop chip level cooling systems to meet heat fluxes in excess of $1000\text{W}/\text{cm}^2$. As stated by Phelan et al [1], "Calculations indicate that the only possible approach to meeting this heat flux condition, while maintaining the chip temperature below 65°C , is to utilize refrigeration." While research has focused on achieving heat transfer rates at the chip level, the resistance to heat transfer to ambient air is often more critical [2]. In fact, the heat transfer resistance to ambient air as the final heat sink is the dominating factor in system performance. Certain classes of components such as field programmable gate arrays, diode lasers and mobile network systems are being deployed in environments where passive

cooling systems cannot maintain junction temperatures below required upper limits. Programs such as the US Army's Warfare Information Network-Tactical (WIN-T) fall into this category [3]. These factors place additional constraints on designers to meet the thermal management challenges of their electronics systems.

PASSIVE VERSUS ACTIVE COOLING SYSTEMS

Passive cooling will be defined herein as a cooling approach that cannot achieve an electronic system operating temperature at or below ambient temperature. In contrast, active cooling systems use added energy to drive the electronic system temperature below that achieved by passive means.

In passively cooled systems, the electronics temperature will rise until the enclosure interface with the ultimate heat sink, usually ambient air, warms up enough to dissipate the heat to the environment as shown in the left half of Figure 1. Methods to reduce the internal temperature rise in these systems include liquid coolant loops, pumped

phase change systems, high conductivity chassis and heat pipes. Although these methods reduce the resistance to internal heat transfer, they do not help overcome the thermal resistance associated with the transport of heat to the ambient air. Fan cooling aides in heat transfer to air by increasing convection, but this approach cannot lower the enclosure surface below the ambient air temperature. As a result, passively cooled electronics used in high temperature ambient environments run at high temperature, sometimes above recommended operational limits.

Active cooling uses energy to lower the electronics temperature to acceptable levels as illustrated in the right half of Figure 1. Active cooling systems raise the temperature of the surfaces exposed to air, increasing heat transfer to the air, while simultaneously lowering the temperature of the surfaces exposed to the electronics, thereby increasing heat transfer on both sides of the system. The major advantage of active cooling is that desired chip junction temperatures can be maintained independently of the ambient air temperature. The disadvantage is that additional power is required to accomplish this task. Therefore, the packaging engineer should use passive cooling techniques only in ambient conditions suitable for passive cooling and use active techniques under all other ambient conditions.

The maximum allowable junction temperature ($T_{j_{\max}}$) is provided by the manufacturer. To determine the junction temperature in the system (T_j),

James Burnett is the director of Government Business Development at Aspen Systems Inc. Burnett has over 30 years of experience as an engineer, program manager and technologist, developing materials and processes for applications that provide structural and thermal solutions for electronic packaging engineers. Activities include developing polymer and metal matrix composite materials and processing and structural designs that enable effective thermal management in high temperature devices. His recent focus has been identifying applications and designs for active cooling of electronics using Aspen's unique miniature refrigeration technology.



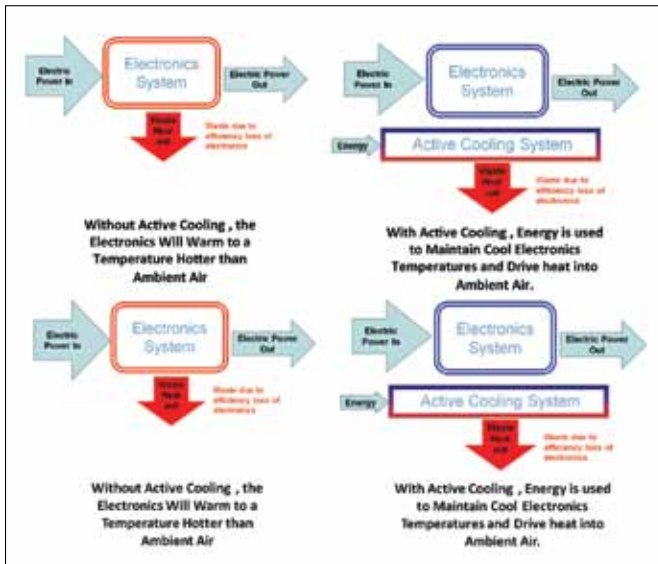


FIGURE 1: Passive and Active Electronics Cooling.

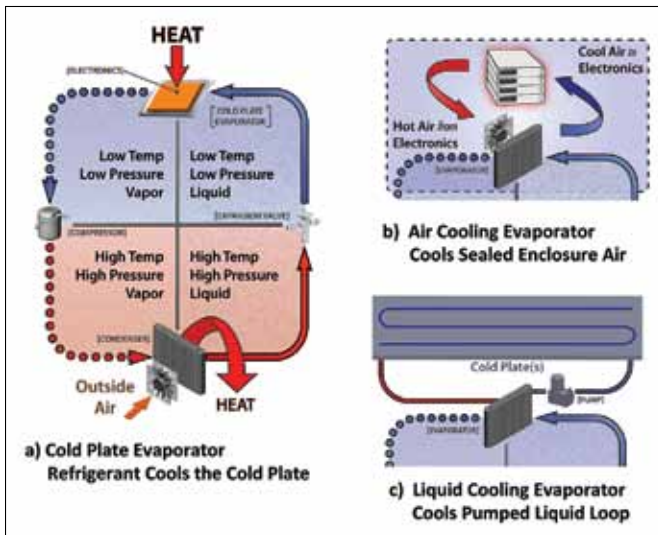


FIGURE 3: Vapor Compression System Schematic.

the sum of the ambient air temperature, the temperature rise from air to the package and the conductive temperature rise internal to the package are calculated. If $T_j \geq T_{j,max}$, then an active cooling system is required. If $T_j \leq T_{j,max}$, then a passive system is sufficient. The decision path to determine the need for active cooling is shown in the flow chart in Figure 2.

The least costly and most efficient time to address such thermal management issues is during the concept development phase of the program. Applying these decision process steps early in the effort can clarify and simplify discussions with program managers and customers, enabling effective thermal management solutions to receive the attention required.

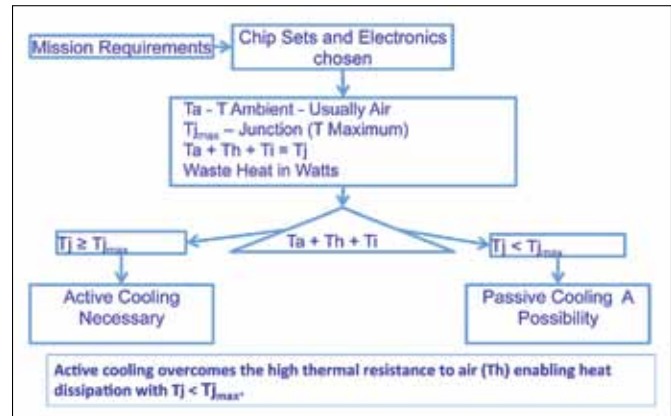


FIGURE 2: Active-Passive cooling decision flow path.



FIGURE 4: Miniature Compressor is 1/10th the Volume and Weight of Conventional Systems.

ACTIVE COOLING METHODS

There are several technologies that can be used for active cooling of electronics systems. Government studies have included thermoelectric, thermotunneling, magnetic and others in their comparisons. The general consensus is that vapor compression is more efficient and lighter than alternative technologies in most applications. A Department of Energy-sponsored study carried out in 2010 [4], compared vapor compression systems with five competing technologies including thermoelectric, thermoacoustic and magnetic technologies. The study focused primarily on efficiency and concluded that vapor compression systems are at least three times more efficient than all available alternatives. An earlier study conducted by the Environmental Protection Agency [5], concluded that "vapor compression refrigeration using non-CFC refrigerants is the most desirable technology of those considered for use in the five application areas considered in this study (domestic, commercial, and mobile air conditioning; and domestic and commercial refrigeration). This conclusion is supported by the first place ranking that vapor compression received in the technical assessment of each technology."



FIGURE 5: Components in a Miniature Refrigeration System.

Vapor Compression System Options

Vapor compression systems take advantage of the latent heat of vaporization of liquids that have a boiling point lower than the desired temperature to be managed. The four major elements of the system are the compressor, condenser, expansion valve, and evaporator, as shown in Figure 3a. In the evaporator, the refrigerant vaporizes at a low temperature, absorbing heat from the electronics. At the evaporator, the refrigerant is a low temperature vapor, as shown in the upper left quadrant of the vapor cycle diagram. The vapor then passes through the compressor,

where it is brought to high pressure and a temperature typically 10°C to 15°C higher than ambient. This hot vapor is converted to liquid in the condensing heat exchanger where heat is rejected to ambient air. The hot liquid refrigerant then exits the condenser and passes through an expansion valve, dropping the refrigerant to a low pressure and temperature. The low-temperature, low-pressure liquid refrigerant then enters the evaporator and the cycle begins again.

Vapor compression environmentally controlled units (ECUs) are routinely customized to meet the specific requirements of an integrated design. Three evaporator options available for vapor compression systems include direct expansion, air cooling, and secondary liquid loop as shown in Figure 3.

The direct expansion option is shown with the complete vapor compression schematic in Figure 3a. With no separate fans or pumps on the evaporator side of the system, this approach has the advantage of relatively few components for light weight and simplicity, and is the most efficient of the three options. The disadvantage of this approach is that the cold plates and the condenser need to be in close proximity to one another to be effective.

The liquid cooled system shown in Figure 3c uses an evaporator that cools a pumped liquid, typically glycol and water. The coolant is passed to a cold plate to remove heat from the electronics. This approach has the advantage that the refrigeration system can be remotely located from the system to be cooled, and disconnected in the field if desired. The disadvantage of this system is the additional temperature rise at the evaporator, and the line losses that can be expected if the refrigeration unit is a great distance from the thermal load.


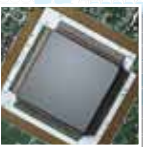


The air cooling refrigeration system uses a refrigerant to air heat exchanger as shown in the upper right quadrant of Figure 3b. Fans are used to move air through the evaporator and circulate the chilled air across the electronics in the enclosure. This method is used when rack mounted electronics are placed in outdoor environments and need to be protected from the elements and from heat.




MINIATURE VAPOR COMPRESSION SYSTEM TECHNOLOGY


The main barrier to using vapor compression cooling systems at the enclosure level has been the availability of refrigeration

THERMAL INTERFACE MATERIALS

HIGH PERFORMANCE & LOW COST OPTIONS
FROM 1 to 17Watt/M-K!



For Technical Data, Samples, Engineering Support
Get Our Catalog, Visit Our Site www.fujipoly.com or
Call 732.969.0100

compressors small enough for the application. In 2007, a miniature refrigeration compressor came onto the market and is now being used in applications ranging from mobile military electronics to laser cooling on manufacturing floors. This compressor and the first prototype experimental cooling systems utilizing it were introduced in an article in the May 2008 issue of *Electronics Cooling*.

The compressor shown in Figure 4 was developed specifically to enable the miniaturization of vapor compression cooling systems for personnel and electronics cooling. This miniature compressor is one-tenth the weight and one-tenth the volume at the same capacity as a competing standard reciprocating compressor. This is the key enabling component in miniature refrigeration systems with cooling requirements up to about 1,000 watts.

Vapor Compression System Components

Other enabling miniaturized components include controllers and drive boards that are designed to meet electromagnetic interference (EMI) requirements are shown in the left picture of Figure 5 along with a direct expansion evaporator, shown in the middle picture, and an aluminum condenser and air evaporator with microchannels as shown in the right picture.

COOLING SYSTEM EXAMPLES

Examples of direct refrigerant, liquid cooling and air cooling vapor compression systems are shown in Figure 6. The direct refrigerant cooling system (Figure 6a) is for an industrial application. The liquid cooling system (Figure 6b) is a military hardened liquid chiller. This system uses two-phase evaporative cooling on the cold plate to efficiently remove heat from a pumped diode laser. The liquid cooling system is a military hardened liquid chiller that was designed, developed and is now in initial production for applications with the US Army. It provides 350 watts of cooling to a cold plate via a pumped water glycol solution. The system measures 27.9 cm (11 in) by 21 cm (8.25 in) by 14 cm (5.5 in) and weighs 5.44 kg (12 lbs).

The air cooling system shown in Figure 6c is a ruggedized vapor compression cooling/heating system designed specifically to meet military requirements for harsh, high vibration environments. This system has been in service on multiple Department of Defense programs. Most notably, over 1,000 of these systems have been in use on Special Operations Command (SOCOM) Mine Resistant, Ambush Protected (MRAP) vehicles for nearly three years.

The air flow patterns for the condenser on the outside surface (left) and evaporator (right) inside the enclosure are shown in Figure 7. The unit maintains a sealed electronics enclosure at or below ambient temperature, enabling Commercial Off-The-Shelf (COTS) electronics to be safely and effectively used in hot, dirty environments.

The unit is rated to maintain an internal temperature of 52°C (125°F) in an ambient environment at 52°C (125°F) while dissipating 550 watts of heat. In cold environments, the ECU heats the electronics from as low as -40°C to preheat the system for cold starts. The system weighs 9.1 kg (20 pounds) and measures



FIGURE 6: Direct, Liquid, and Air Cooling Vapor Compression Systems: (from top) a) Direct Refrigerant System; b) Liquid Chiller System; c) Air Chiller System.

47 cm (18.5 in) wide by 22.9 cm (9 in) tall by 17cm (6.7 in) deep.

CONCLUSION

Miniature vapor compression thermal management systems are being custom designed to meet Original Equipment Manufacturer (OEM) and end user specifications for a wide array of electronics thermal management applications. A transit case cooling system has been developed and refined to meet stringent military program requirements for mobile network applications and is currently operating worldwide. A liquid chiller system has been developed for use on radio and computer cooling in mobile environments and several direct refrigerant systems have been developed for end users and OEMs. An airborne cooling system was developed to meet mission critical requirements for cooling infrared cameras. Miniature refrigeration technology is now mature, qualified and fielded for effective application to electronics systems that require active cooling.

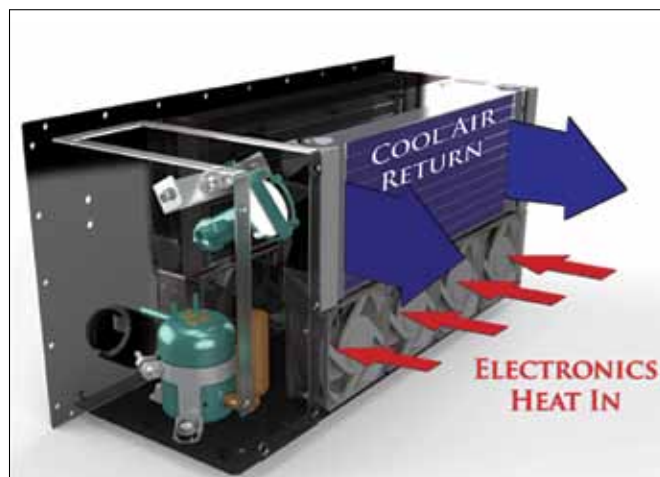


FIGURE 7: Air Flow Patterns Outside (Left) and Inside (Right) the Air Cooling Environmental Control Unit.

REFERENCES

[1] "Energy Efficiency of Refrigeration Systems for High-Heat-Flux Micro-electronics"

P. E. Phelan, J. Catano, G. Michna, Y. Gupta, H. Tyagi, R. Zhou, J. Wen, R. S.

Prasher, M. Jensen and Y. Peles J. Thermal Sci. Eng. Appl. 2(3), 031004 (Dec 16, 2010) (6 pages) doi:10.1115/1.4003041

[2] "Current and Future Miniature Refrigeration Cooling Technologies for High Power Microelectronics" Patrick E. Phelan, Victor A. Chiriac, and Tien-Yu Tom Lee, Associate Member, IEEE, IEEE TRANSACTIONS ON COMPONENTS AND PACKAGING TECHNOLOGIES, VOL. 25, NO. 3, SEPTEMBER 2002 pp 356-365.

[3] Authors Personal Experience with the Warfare Information Network-Tactical Program

[4] "The Prospects of Alternatives to Vapor Compression Technology for Space Cooling and Food Refrigeration Applications", DR Brown, N Fernandez, JA Dirks, TB Stout, Department Of Energy Report No. PNNL-19259, Prepared under contract No Contract DE-AC05-76RL01830 March 2010

[5] "Alternative Technologies for Refrigeration and Air-Conditioning Applications" D.C. Gauger, N. Shapiro, and M.B. Pate, ' =Research and Development EP/600/SR-95/066 May 1995

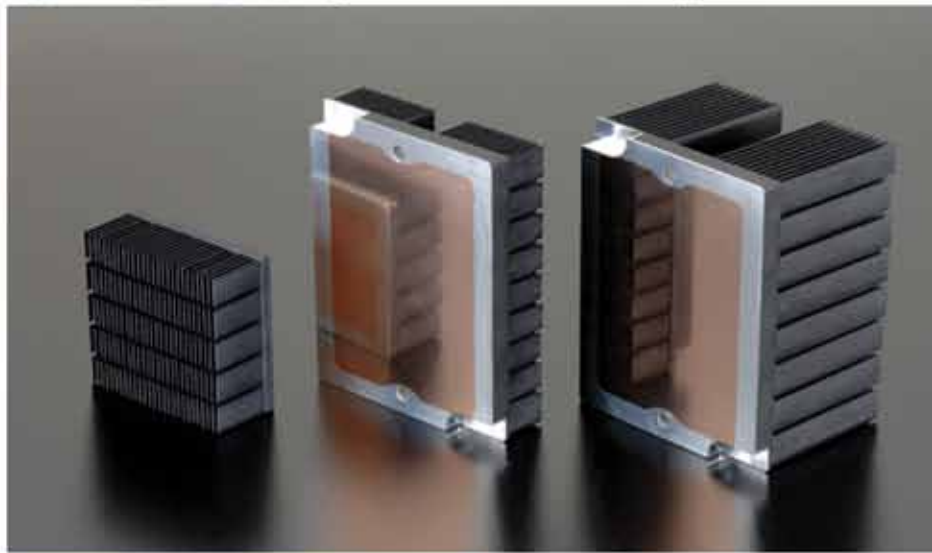
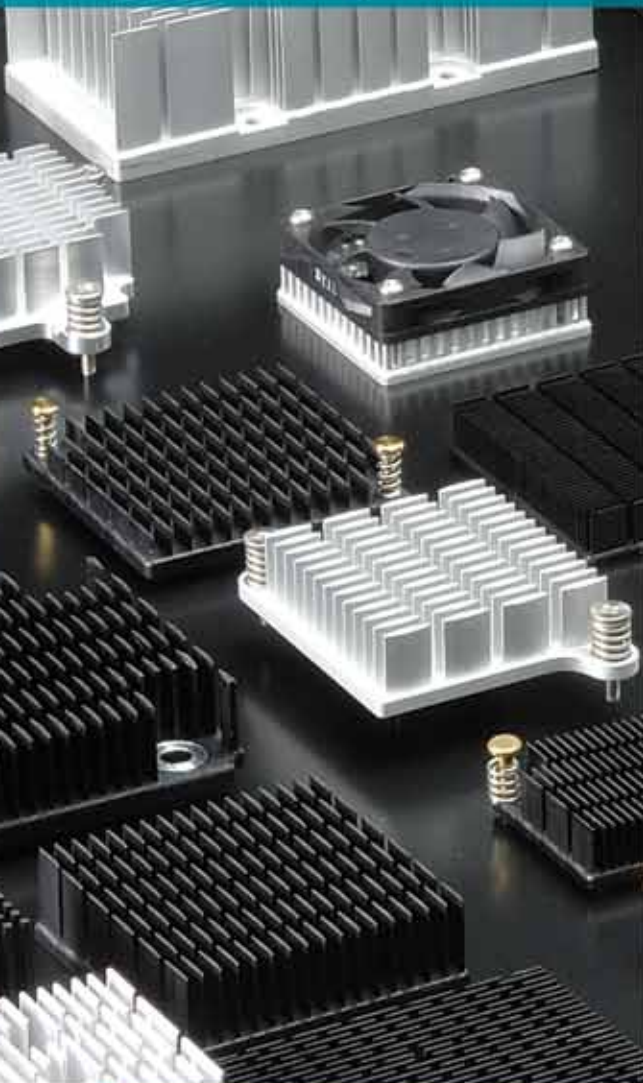
[6] "2U Rack Mountable Vapor Compression Cooling System For High Power Electronics" G. Deming, Electronics Cooling, May 2008.

Index of Advertisers

Alpha Novatech, Inc.....	Inside Back Cover
The Bergquist Company.....	Inside Front Cover
Electronic Components and Technology Conference (ECTC).....	23
EMC LIVE	32
Fujipoly America Corp.....	30
Kunze Folien GmbH.....	17
Malico Inc.....	3
Mentor Graphics	27
Rogers Corporation.....	11
SEMI-THERM.....	15
Sapa Extrusions North America	9
Summit Thermal System Co. Ltd.....	16
Sunon Inc.	Back Cover

Alpha's Next Generation Heat Sink

Custom or off-the-shelf.
Simple to complex.
Prototype to mass production.



Quick and Simple



Online Heat Sink Customization

Custom heat sinks do not have to be an expensive luxury. Alpha can produce custom parts in small lots at a very reasonable cost. This is made possible by our large variety of catalog heat sinks and our flexible manufacturing process.

Minimum Order Quantity : 1 piece
Average Lead-Time : 5 days
Instant / Rapid Quote
Thermal / Mechanical Support

ALPHA ONLINE SERVICES

Online Catalog

Over 1,000 items with a variety of options!

Data Library

Download 2D/3D CAD files, Flotherm data, RoHS/REACH CoC and more.

Online Shopping :

Most catalog parts are carried in stock!

Heat sink Selection Service

Online service collects pertinent application data that will streamline the heat sink selection process.

ALPHA

Your partner for thermal solutions

ALPHA Co., Ltd.
Head Office
www.micforg.co.jp

ALPHA NOVATECH, INC.
USA Subsidiary
www.alphanovatech.com

256-1 Ueda, Numazu City, Japan 410-0316
Tel: +81-55-966-0789 Fax: +81-55-966-9192
Email: alpha@micforg.co.jp

473 Sapena Ct. #12, Santa Clara, CA 95054 USA
Tel: +1-408-567-8082 Fax: +1-408-567-8053
Email: sales@alphanovatech.com

Dustproof

Harsh Environment IP68 cooling Fan



Waterproof

Harsh Environment IP68 cooling Fan



SUNON®

Sunonwealth Electric Machine Industry Co., Ltd

Headquarters (Taiwan) URL : www.sunon.com
Sunon Inc. (U.S.A.) E-mail : info@sunon.com | Tel : +1-714-255-0208

©2014 SUNONWEALTH Electric Machine Industry Co., Ltd

